

49p.

Ag 19

MSFC
MTP-AERO-62-19
March 6, 1962

OTS: \$



N64-15887

CODE-1

NASA TMX-54568;

NASA.

GEORGE C. MARSHALL

**SPACE
FLIGHT
CENTER,**

HUNTSVILLE, ALABAMA

THE LOW AND THE HIGH PRANDTL NUMBER APPROACHES FOR HEAT TRANSFER IN
LAMINAR FLOW OF INCOMPRESSIBLE FLUIDS
WITH CONSTANT MATERIAL PROPERTIES

By

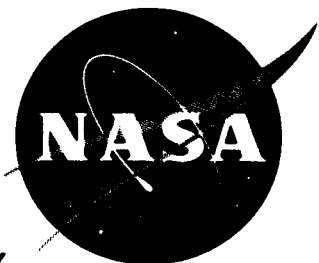
Ernst W. Adams

PROPERTY OF
TECHNICAL LIBRARY
M-MS-IPL

6 Mar. 1962 49p refs

OTS PRICE

XEROX \$ 4.60 ph
MICROFILM \$ 1.67 mf.



FOR INTERNAL USE ONLY

SCIENTIFIC AND SPACE ADMINISTRATION

GEORGE C. MARSHALL SPACE FLIGHT CENTER

MTP-AERO-62-19

THE LOW AND THE HIGH PRANDTL NUMBER APPROACHES FOR HEAT TRANSFER IN
LAMINAR FLOW OF INCOMPRESSIBLE FLUIDS
WITH CONSTANT MATERIAL PROPERTIES

ERNST W. ADAMS

ABSTRACT

Exact closed form solutions of the boundary layer equations can be derived for the Nusselt number $Nu(x)$ at the leading edge $x = 0$ and, in the limits $Pr \rightarrow 0$ and $Pr \rightarrow \infty$, on the surface $x \geq 0$ of arbitrary bodies in planar uniform flow. Published results of exact and of approximate solutions for $Nu(x)/Nu(0)$ in the range $0 < Pr < \infty$ are compared to the results of the $Pr \rightarrow 0$ and the $Pr \rightarrow \infty$ methods. The $Pr \rightarrow 0$ method yields an upper limit for $Nu(x)/Nu(0)$. The presented examples show that the $Pr \rightarrow \infty$ method yields a lower limit for $Nu(x)/Nu(0)$ in case of slender bodies. Both methods yield the exact solution for $Nu(x)/Nu(x^*)$ in the cases for which similarity solutions exist. The $Pr \rightarrow 0$ and the $Pr \rightarrow \infty$ methods are applicable to obtain engineering estimates of heat transfer.

GEORGE C. MARSHALL SPACE FLIGHT CENTER

MTP-AERO-62-19

March 6, 1962

THE LOW AND THE HIGH PRANDTL NUMBER APPROACHES FOR HEAT TRANSFER IN
LAMINAR FLOW OF INCOMPRESSIBLE FLUIDS
WITH CONSTANT MATERIAL PROPERTIES

by

Ernst W. Adams

AERODYNAMICS ANALYSIS BRANCH
AEROBALLISTICS DIVISION

ACKNOWLEDGEMENT

The author wishes to acknowledge the very conscientious assistance of Mr. C. Lee Fox in preparing the material presented in this paper.

TABLE OF CONTENTS

	Page
LIST OF ILLUSTRATIONS.....	iv
LIST OF SYMBOLS.....	vi
SUMMARY.....	1
I. INTRODUCTION.....	1
II. THE LOW PRANDTL NUMBER METHOD.....	2
III. APPLICATION OF THE LOW PRANDTL NUMBER METHOD TO CASES FOR WHICH SIMILARITY SOLUTIONS EXIST.....	5
IV. THE HIGH PRANDTL NUMBER METHOD.....	7
V. APPLICATION OF THE HIGH PRANDTL NUMBER METHOD TO CASES FOR WHICH SIMILARITY SOLUTIONS EXIST.....	8
VI. THE FUNCTIONS $u_e(x)$ AND $c_f(x)$ FOR THE INVESTIGATED CASES...	9
VII. DISCUSSION OF THE RESULTS.....	11
VIII. CONCLUSIONS.....	12
APPENDIX.....	14
REFERENCES.....	36
APPROVAL.....	38
DISTRIBUTION.....	39

LIST OF ILLUSTRATIONS

Figure	Title	Page
1.	Non-Dimensional Wall Temperature Gradient for Flat Plate.....	17
2.	Non-Dimensional Friction Coefficient from Exact Similarity Solutions.....	18
3.	$Nu_2(x) / \sqrt{Re_2(x)}$ from Exact Similarity Solutions.....	19
4.	$Nu_2(x) / \sqrt{Re_2(x)Pr}$ for Flat Plate.....	20
5.	Circular Cylinder in Uniform Planar Flow in the $\xi_0-\eta_0$ Plane.....	21
6.	Elliptical Cylinder in Uniform Planar Flow in the $\xi_1-\eta_1$ Plane.....	21
7.	Velocity Distributions at Surfaces of Circular and Elliptic Cylinders.....	22
8.	Velocity Distributions at Surface of Airfoil.....	23
9.	Friction Coefficient for Flat Plate, Circular, and Elliptic Cylinder.....	24
10.	$Nu_1(x)/Nu_1(0)$ for Elliptical Cylinder 1 : 4, $T_w = \text{const}$	25
11.	$Nu_1(x)/Nu_1(0)$ for Elliptical Cylinder 1: 2, $T_w = \text{const}$	26
12.	$Nu_1(x)/Nu_1(0)$ for Elliptical Cylinder 1 : 1.5, $T_w = \text{const}$	27
13.	$Nu_1(x)/Nu_1(0)$ for Circular Cylinder, $T_w = \text{const}$	28
14.	$Nu_1(x)/Nu_1(0.1)$ for Single Airfoil, $T_w = \text{const}$	29
15.	$Nu_1(x)/Nu_1(0.1)$ for Airfoil in Cascade, $T_w = \text{const}$...	30
16.	$Nu_1(x)/Nu_1(0)$ for Elliptical Cylinder 1 : 4, $T_w \neq \text{const}$	31
17.	$Nu_1(x)/Nu_1(0.2)$ for Flat Plate, $T_w \neq \text{const}$	32
18.	$Nu_3(x)/Nu_3(0)$ for Flat Plate, $T_w \neq \text{const}$	33

LIST OF ILLUSTRATIONS (CONT'D)

19.	$Nu_1(x) / \sqrt{Re_1}$ for Elliptical Cylinder 1 : 4, $T_w = \text{const} \dots \dots \dots$	34
20.	$Nu_1(x) / \sqrt{Re_1}$ for Circular Cylinder, $T_w = \text{const} \dots \dots \dots$	35

DEFINITION OF SYMBOLS

$A = \frac{k}{\rho g c_p}$	m^2/sec	Thermal diffusivity
$c = du_e(0)/dx$	$1/sec$	Velocity gradient at stagnation point
c_f		Wall friction coefficient
c_p	$kcal/kg \text{ } ^\circ K$	Specific heat
C		Constant in the equation (19)
g	m/sec^2	Gravity constant
k	$kcal/m \text{ } ^\circ K \text{ sec}$	Thermal conductivity
L	m	Reference length
m and n		Exponents in the equation (19)
$Nu_1 = \frac{Lq_w(x)}{k[T_w(0)-T_o]}$		Nusselt number defined in the equation (15)
$Nu_2 = \frac{xq_w(x)}{k[T_w(x)-T_o]}$		Nusselt number defined in the equation (20)
$Pr = \frac{\mu g c_p}{k}$		Prandtl number
p	kg/m^2	Pressure
q_w	$kcal/m^2 \text{ sec}$	Wall heat transfer
R	m	Radius, Fig. 5
$Re_1 = \frac{L\rho u_\infty}{\mu}$		Reynolds number defined in the equation (13)
$Re_2 = \frac{x\rho u_e(x)}{\mu}$		Reynolds number defined in the equation (20)
T	$^\circ K$	Temperature
T_o	$^\circ K$	Constant temperature at outer edge of boundary layer

DEFINITION OF SYMBOLS (Cont'd)

T_w	$^{\circ}\text{K}$	Wall temperature
u	m/sec	Velocity component in x-direction
u_e	m/sec	Velocity at outer edge of boundary layer
u_{∞}	m/sec	Speed of ambient uniform flow
v	m/sec	Velocity component in y-direction
x	m	Coordinate measuring parallel to wall
x^*	m	Reference value on x-scale
y	m	Coordinate measuring normal to wall
δ_t	m	Thickness of thermal boundary layer
δ_v	m	Thickness of velocity boundary layer
φ		Angle, Fig. 5
\varnothing	m^2/sec	Velocity potential
ψ	m^2/sec	Stream function
ρ	$\text{kg sec}^2/\text{m}^4$	Density
μ	$\text{kg sec}/\text{m}^2$	Viscosity
ξ	m	Dummy variable for x
η	m^2/sec	Dummy variable for \varnothing

MTP-AERO-62-19

THE LOW AND THE HIGH PRANDTL NUMBER APPROACHES FOR HEAT TRANSFER IN
LAMINAR FLOW OF INCOMPRESSIBLE FLUIDS WITH
CONSTANT MATERIAL PROPERTIES

by Ernst W. Adams

SUMMARY

Exact closed form solutions of the boundary layer equations can be derived for the Nusselt number $Nu(x)$ at the leading edge $x = 0$ and, in the limits $Pr \rightarrow 0$ and $Pr \rightarrow \infty$, on the surface $x \geq 0$ of arbitrary bodies in planar uniform flow. Published results of exact and of approximate solutions for $Nu(x)/Nu(0)$ in the range $0 < Pr < \infty$ are compared to the results of the $Pr \rightarrow 0$ and the $Pr \rightarrow \infty$ methods. The $Pr \rightarrow 0$ method yields an upper limit for $Nu(x)/Nu(0)$. The presented examples show that the $Pr \rightarrow \infty$ method yields a lower limit for $Nu(x)/Nu(0)$ in case of slender bodies. Both methods yield the exact solution for $Nu(x)/Nu(x^*)$ in the cases for which similarity solutions exist. The $Pr \rightarrow 0$ and the $Pr \rightarrow \infty$ methods are applicable to obtain engineering estimates of heat transfer.

15887

Author

I. INTRODUCTION

The problem of the stationary heat exchange between the impermeable wall of an arbitrary body in planar uniform and laminar flow with negligible frictional heating of an incompressible fluid with constant material properties is encountered in many engineering applications. The mathematical treatment of this problem starts from the equations of continuity, momentum, and energy. The boundary layer versions of the equations of momentum and energy may be employed when both the Reynolds number $Re = L_0 u_\infty/\mu$ and the Peclet number $Pe = Re Pr$ are sufficiently large, where $Pr = \mu g c_p/k$ is the Prandtl number. Exact solutions of this boundary layer problem are presented in references 2, 5, 8, 10, 13, 16, and 22. Integral solutions of the Kármán-Pohlhausen type are presented in references 4, 17, and 23. The energy equation for the temperature distribution in the boundary layer is a linear second-order differential equation, which can be integrated analytically only in special cases because of the explicit occurrence of the velocity components $u(x,y)$ and $v(x,y)$ as coefficients in this equation. The integration becomes generally feasible in the limiting cases $Pr \rightarrow 0$ and $Pr \rightarrow \infty$.

The process $Pr \rightarrow 0$ is compatible with the before-mentioned condition $Pe = Re Pr = (u_\infty L)(\rho g c_p/k) \gg 1$ if it is accomplished by $\mu \rightarrow 0$,

i.e., by the substitution of an ideal fluid for the given real fluid. If δ_v is the thickness of the velocity boundary layer and if δ_t is the thickness of the temperature boundary layer, $\lim_{Pr \rightarrow 0} \frac{\delta_v}{\delta_t} = 0$ and $\lim_{Pr \rightarrow \infty} \frac{\delta_t}{\delta_v} = 0$.

The velocity distribution throughout the temperature boundary layer, therefore, may be replaced for $Pr \rightarrow 0$ by the velocity distribution $u_e(x)$ at the outer edge of the boundary layer, which is a result of ideal fluid theory. Also, the velocity distribution throughout the temperature boundary layer may be replaced by the wall tangent $u = y\tau_w(x)/\mu$ for $Pr \rightarrow \infty$, where τ_w is the wall shear stress.

Lighthill presented in reference 12 an exact analysis for the approach $Pr \rightarrow \infty$. References 3, 11, and 20 treat approximately valid extensions of Lighthill's "High Prandtl Number Method" by the inclusion of a quadratic term in the expression for $u(x,y)$. The apparently first application of the approach $Pr \rightarrow 0$ appeared on pp. 597 - 600 of reference 7. Reference 14 presents the basic equations for the "Low Prandtl Number Method," $Pr \rightarrow 0$, and the equations for a first-order correction as part of a series expansion in terms of powers of Pr . The very involved correction terms are worked out in reference 14 only for power laws representing the speed $u_e(x)$ at the outer edge of the boundary layer and the wall temperature $T_w(x)$. The Fig. 1, which is taken from reference 14, shows for constant wall temperature and zero pressure gradient that the first-order correction improves the results of the approach $Pr \rightarrow 0$ only for $Pr < 0.1$.

Since only a few comparative evaluations of the $Pr \rightarrow 0$ and the $Pr \rightarrow \infty$ methods and of exact or approximate solutions for $0 < Pr < \infty$ have been published, such a comparison is presented here by employing all the solutions for $0 < Pr < \infty$ which are known to the author.

II. THE LOW PRANDTL NUMBER METHOD

The boundary layer problem under consideration is governed by the three differential equations

$$\frac{\partial u}{\partial x} + \frac{\partial v}{\partial y} = 0, \quad \text{continuity equation,} \quad (1)$$

$$u \frac{\partial u}{\partial x} + v \frac{\partial u}{\partial y} = -\frac{1}{\rho} \frac{dp}{dx} + \frac{\mu}{\rho} \frac{\partial^2 u}{\partial y^2}, \quad \text{momentum equation, and} \quad (2)$$

$$u \frac{\partial T}{\partial x} + v \frac{\partial T}{\partial y} = \frac{k}{\rho g c_p} \frac{\partial^2 T}{\partial y^2}, \quad \text{energy equation,} \quad (3)$$

which are taken from p. 136/37 of reference 15. The continuity equation (1) can be satisfied by a stream function ψ so that

$$\frac{\partial \psi(x,y)}{\partial y} = u(x,y) \quad \text{and} \quad \frac{\partial \psi(x,y)}{\partial x} = -v(x,y). \quad (4)$$

The von Mises transformation is introduced in order to replace x and y by φ and $\psi(x, y)$ in the energy equation (3). If the derivative with respect to x when y is constant is denoted by $(\partial/\partial x)_y$, with a similar notation for other derivatives, the following transformation formulae are now derived, p. 152 of reference 15:

$$\begin{aligned} \left(\frac{\partial}{\partial x}\right)_y &= \left(\frac{\partial}{\partial \varphi}\right)_\psi + \left(\frac{\partial}{\partial \psi}\right)_x \left(\frac{\partial \psi}{\partial x}\right)_y = \left(\frac{\partial}{\partial \varphi}\right)_\psi - v \left(\frac{\partial}{\partial \psi}\right)_x \quad \text{and} \\ \left(\frac{\partial}{\partial y}\right)_x &= \left(\frac{\partial}{\partial \psi}\right)_x \left(\frac{\partial \psi}{\partial y}\right)_x = u \left(\frac{\partial}{\partial \psi}\right)_x \end{aligned} \quad (5)$$

The relations (3) and (5) yield the equation

$$\frac{\partial T}{\partial \varphi} = \frac{k}{\rho g c_p} \frac{\partial}{\partial \psi} \left[u \frac{\partial T}{\partial \psi} \right] \quad (6)$$

As $Pr \rightarrow 0$ through $\mu \rightarrow 0$, the energy equation (6) may be replaced by

$$\frac{\partial T}{\partial \varphi} = \frac{k}{\rho g c_p} \frac{\partial^2 T}{\partial \psi^2}, \quad \text{where } \varphi(x) = \int_0^x u_e(x) dx \quad (7)$$

because of $\lim_{\mu \rightarrow 0} u(x, \psi) = u_e(x)$. The following initial and boundary conditions are assumed for the solution of the energy equation (7):

$$T(0, \psi) = T_0 = \text{const.} \quad \text{at the leading edge } \varphi = x = 0, \quad (8)$$

$$T(\varphi, 0) = T_w(\varphi) \quad \text{at the wall } \psi = 0, \text{ and} \quad (9)$$

$$\lim_{\psi \rightarrow \infty} T(\varphi, \psi) = T_\infty = \text{const.} \quad \text{at the outer edge of the boundary layer,} \quad (10)$$

where $T_w(\varphi)$ is a given continuously differentiable function of φ .

Equations (7) through (10) determine a problem of the type of transient one-dimensional heat conduction. The application of pertinent solution methods in reference 1 yields the equation (A-13) in the appendix

$$q_w(x) = \sqrt{\frac{k \rho g c_p}{\pi}} u_e(x) \left[\frac{T_w(0) - T_o}{\sqrt{\phi(x)}} + \int_{\eta=0}^{\eta=\phi(x)} \frac{dT_w(\eta)}{d\eta} \frac{d\eta}{\sqrt{\phi(x) - \eta}} \right] \quad (11)$$

for the heat transfer rate $q_w(x) = -k \partial T(x, 0) / \partial y$ at the wall $y = 0$. Since $d\phi(x)/dx = u_e(x) > 0$ between the forward stagnation point $x = 0$ and the rear stagnation point, equation (11) may be replaced by

$$q_w(x) = \sqrt{\pi^{-1} \left(\frac{\mu g c_p}{k} \right) \left(\frac{L \rho u_\infty}{\mu} \right)} \frac{k}{L} [T_w(0) - T_o] \frac{u_e(x)}{u_\infty} \left[\frac{1}{\sqrt{\frac{\phi(x)}{u_\infty L}}} + \int_{\xi=0}^{\xi=L} \frac{d \frac{\xi}{L}}{d \frac{\xi}{L}} \left(\frac{T_w(\xi) - T_o}{T_w(0) - T_o} \right) \frac{d \frac{\xi}{L}}{\sqrt{\frac{\phi(x) - \phi(\xi)}{u_\infty L}}} \right] \quad (12)$$

The following definitions of the Reynolds number, Prandtl number, and Nusselt number are employed:

$$Re_1 = \frac{L \rho u_\infty}{\mu}, \quad (13)$$

$$Pr = \frac{\mu g c_p}{k}, \text{ and} \quad (14)$$

$$Nu_1(x) = \frac{L q_w(x)}{k [T_w(0) - T_o]} \quad (15)$$

According to p. 70 reference 19,

$$\frac{u_e(x)}{u_\infty} = c \frac{x}{L} \quad \text{with } c = \text{const.} \quad (16)$$

in a small vicinity of the forward stagnation point, i.e.,

$$\lim_{x \rightarrow 0} \frac{u_e(x)/u_\infty}{\sqrt{\phi(x)/u_\infty L}} = \sqrt{2c} \text{ and } Nu_1(0) = \sqrt{Re_1 Pr \frac{2c}{\pi}}. \quad (17)$$

Thus the following relation can be derived:

$$\frac{Nu_1(x)}{Nu_1(0)} = \frac{1}{\sqrt{2c}} \left[\frac{\frac{u_e(x)}{u_\infty}}{\sqrt{\frac{\phi(x)}{u_\infty L}}} + \frac{u_e(x)}{u_\infty} \int_{\xi=0}^{\xi=x} \frac{d \frac{\xi}{L}}{d \frac{\xi}{L}} \left(\frac{T_w(\xi) - T_o}{T_w(0) - T_o} \right) \frac{d \frac{\xi}{L}}{\sqrt{\frac{\phi(x) - \phi(\xi)}{u_\infty L}}} \right] \quad (18)$$

III. APPLICATION OF THE LOW PRANDTL NUMBER METHOD TO CASES FOR WHICH SIMILARITY SOLUTIONS EXIST

Similarity solutions of the boundary layer equations (1) through (3) exist in case of constant material properties and if

$$\frac{u_e(x)}{u_{\infty}} = C \left(\frac{x}{L}\right)^m \text{ and } T_w(x) - T_o = \begin{cases} T_o D \left(\frac{x}{L}\right)^n & \text{for } n \neq 0, \text{ or} \\ T_w(0) - T_o = \text{const}, & \end{cases} \quad (19)$$

where C, D, m, and n are constant numbers and the Prandtl number is arbitrary. For convenience, the Reynolds number and the Nusselt number are defined here as follows:

$$Re_2(x) = \frac{\rho x u_e(x)}{\mu} \text{ and } Nu_2(x) = \frac{x q_w(x)}{k[T_w(x) - T_o]} \quad (20)$$

Data for $Nu_2(x)/\sqrt{Re_2(x)}$ resulting from exact numerical similarity solutions of the equations (1) through (3) are derived in references 5 and 10 for several sets of values m, n, and Pr. Reference 12 presents additional results for $n = 0$ and $Pr = 0.7$. The data presented in reference 10, which pertains to the ranges $-0.0904 \leq m \leq 4$, $-2.5 \leq n \leq 4$, and $0.7 \leq Pr \leq 20$ can be correlated with a $\pm 5\%$ margin of error by the function

$$\frac{Nu_2(x)}{\sqrt{Re_2(x)}} = Pr^{\lambda(m)} B_o(m, n), \quad (21)$$

where

$$B_o(m, n) = 0.57 (0.205 + \beta)^{0.104} \sqrt{\frac{m+1}{2}} \left(1 + \beta \frac{n}{m}\right)^{0.37 + 0.06\beta}, \quad (22)$$

$$0.254 \leq \lambda(m) \leq 0.367, \text{ and } \beta = 2m/(m+1).$$

Since

$$\phi(x) \equiv \int_0^x u_e(x) dx = \frac{u_{\infty} CL}{m+1} \left(\frac{x}{L}\right)^{m+1}, \quad (23)$$

according to equation (19), equation (11) yields

$$q_w(x) = \frac{k}{x} \left[T_w(0) - T_0 \right] \sqrt{\frac{m+1}{\pi}} \sqrt{\text{Pr Re}_2(x)} \quad (24)$$

for constant wall temperature. The heat transfer parameter then takes the following form:

$$\frac{\text{Nu}_2(x)}{\sqrt{\text{Re}_2(x)}} \equiv \frac{x q_w(x)}{k [T_w(0) - T_0] \sqrt{\text{Re}_2(x)}} = \sqrt{\text{Pr} \frac{m+1}{\pi}}. \quad (25)$$

Equation (11) becomes in case of the power laws (19) for $u_e(x)$ and $T_w(x) - T_0$, i.e., in case of variable wall temperature,

$$q_w(x) = k \sqrt{\frac{\text{Pr Re}_2(x)}{\pi}} \sqrt{\frac{u_e(x)}{x}} \frac{T_w(x) - T_0}{\left(\frac{x}{L}\right)^n} \left(\frac{m+1}{u_{\infty} \text{CL}}\right)^{\frac{n}{m+1}} \int_{\eta=0}^{\eta=\phi(x)} \frac{d}{d\eta} (\eta)^{\frac{n}{m+1}} \frac{d\eta}{\sqrt{\phi(x) - \eta}}. \quad (26)$$

The heat transfer parameter then becomes

$$\frac{\text{Nu}_2(x)}{\sqrt{\text{Re}_2(x)}} = \sqrt{\frac{u_{\infty} \text{CL}}{\pi}} \sqrt{\text{Pr}} \frac{n}{m+1} \left(\frac{m+1}{u_{\infty} \text{CL}}\right)^{\frac{n}{m+1}} \left(\frac{x}{L}\right)^{\frac{m+1}{2} - n} J_1(x), \quad (27)$$

where

$$J_1(x) = \phi(x) \int_{\frac{\eta}{\phi} = 0}^{\frac{\eta}{\phi} = 1} \frac{\left(\frac{\eta}{\phi}\right)^M d\left(\frac{\eta}{\phi}\right)}{\sqrt{\left(1 - \frac{\eta}{\phi}\right) \frac{\eta}{\phi}}} \quad \text{and } M = \frac{n}{m+1} - \frac{1}{2}. \quad (28)$$

The right-hand side of equation (27) is independent of x because of the relations (23) and (28); therefore,

$$\frac{\text{Nu}_2(x)}{\sqrt{\text{Re}_2(x)}} = \text{Pr}^{1/2} B_1(m, n). \quad (29)$$

The function J_1 can be evaluated analytically in closed form when M is a positive integer number, and the following values can be obtained for $B_1(m, n)$ in case of some suitably selected pairs of numbers m and n :

m	0	0.25	1	1	4
n	0.5	1.875	1	3	2.5
$B_1(m,n)$	0.8862	1.4862	1.2533	1.8800	1.9817

IV. THE HIGH PRANDTL NUMBER METHOD

It has been explained before why Lighthill approximates the velocity profile $u(x,y)$ in the limit $Pr \rightarrow \infty$ by the expression

$$u(x,y) = \frac{\tau_w(x)}{\mu} y = \sqrt{\frac{2\tau_w(x)}{\mu}} \sqrt{\psi(x,y)}, \quad (30)$$

where $\psi(x,y) = \int_0^y u(x,y) dy = y^2 \tau_w(x) / 2\mu$. The substitution of the relation

(30) into equation (6) yields

$$\frac{\partial T(x,\psi)}{\partial x} = \frac{k}{\rho g c_p} \sqrt{\frac{2\tau_w(x)}{\mu}} \frac{\partial}{\partial \psi} \left[\sqrt{\psi} \frac{\partial T(x,\psi)}{\partial \psi} \right]. \quad (31)$$

Lighthill has solved this partial differential equation by use of Heaviside's operational method in reference 12 and has obtained the relation

$$q_w(x) \equiv -k \frac{\partial T(x,0)}{\partial y} = k \left(\frac{Pr \rho}{9\mu^2} \right)^{1/3} \frac{\sqrt{\tau_w(x)}}{\left(\frac{1}{3} \right)!} \left[\frac{T_w(0) - T_o}{\left(\int_0^x \tau_w^{1/2}(\xi) d\xi \right)^{1/3}} + \right. \\ \left. + \int_{\xi=0}^{\xi=x} \frac{dT_w(\xi)}{d\xi} \frac{d\xi}{\left(\int_{z=\xi}^{z=x} \tau_w^{1/2}(z) dz \right)^{1/3}} \right]. \quad (32)$$

For a vicinity of the stagnation point, an exact solution of the Navier-Stokes differential equations yields

$$\sqrt{\tau_w(x)} = 1.2326 c^{3/2} \sqrt{\mu \rho} x \quad (33)$$

according to p. 70-73 of reference 19, where $c = du_e(0)/dx$ has been defined in equation (16). If the relations (13) through (15) and the usual definition

$$c_f(x) = \frac{\tau_w(x)}{\rho u_\infty^2/2} \quad (34)$$

of the wall friction coefficient are employed, the following equations can be derived:

$$Nu_1(0) = 0.660 \text{ Pr}^{1/3} \text{Re}_1^{1/2} \sqrt{\frac{cL}{u_\infty}} \quad \text{and} \quad (35)$$

$$\begin{aligned} \frac{Nu_1(x)}{Nu_1(0)} = 0.647 \sqrt{\frac{u_\infty}{cL}} & \left[\frac{\sqrt{c_f(x)\text{Re}_1^{1/2}}}{\left(\int_0^x \sqrt{c_f(\xi)\text{Re}_1^{1/2}} d\frac{\xi}{L} \right)^{1/3}} + \right. \\ & \left. + \sqrt{c_f(x)\text{Re}_1^{1/2}} \int_{\xi=0}^{\xi=x} \frac{d\frac{\xi}{L} \left(\frac{T_w(\xi) - T_o}{T_w(0) - T_o} \right)}{d\frac{\xi}{L}} \frac{d\frac{\xi}{L}}{\left(\int_{z=\xi}^{z=x} \sqrt{c_f(z)\text{Re}_1^{1/2}} d\frac{z}{L} \right)^{1/3}} \right]. \end{aligned} \quad (36)$$

V. APPLICATION OF THE HIGH PRANDTL NUMBER METHOD TO CASES FOR WHICH SIMILARITY SOLUTIONS EXIST

If the velocity distribution (19) is stipulated, the wall shear stress becomes

$$\tau_w(x) = \left(\frac{u_\infty}{L^m} \right)^{3/2} (\rho\mu)^{1/2} f_w''(m) x^{\frac{3m-1}{2}}. \quad (37)$$

Numerical results for the function $f_w''(m)$ have been derived in references 5, 9, and 12 and are represented in figure 2 by disregarding a few inconsistent numbers from reference 9. For constant wall temp., equation (32) then becomes

$$q_w(x) = 0.538 \frac{k}{x} [T_w(0) - T_o] \text{Pr}^{1/3} \text{Re}_2^{1/2}(x) \left[\frac{3}{4} (m+1) f_w''(m) \right]^{1/3} \quad (38)$$

and the heat transfer parameter, which is defined in the relations (20), takes the form

$$\frac{Nu_2(x)}{\sqrt{Re_2(x)}} = 0.538 Pr^{1/3} \left[\frac{3}{4} (m+1) f_w''(m) \right]^{1/3}. \quad (39)$$

Equation (32) becomes in case of the power laws (19) for $u_e(x)$ and $T_w(x)-T_0$, i.e., in case of variable wall temperature,

$$q_w(x) = 0.538 \frac{k}{x} [T_w(x)-T_0] Pr^{1/3} Re_2^{1/2}(x) \left[\frac{3}{4} (m+1) f_w''(m) \right]^{1/3} nx^{-n+\frac{m+1}{4}} J_2(x), \quad (40)$$

where

$$J_2(x) = x^{n-\frac{m+1}{4}} \int_{\frac{\xi}{x}=0}^{\frac{\xi}{x}=1} \left(\frac{\xi}{x} \right)^{n-1} \left[1 - \left(\frac{\xi}{x} \right)^{\frac{3}{4}(m+1)} \right]^{-1/3} d \frac{\xi}{x}. \quad (41)$$

The heat transfer parameter, which is defined in the equations (20), then takes the form

$$\frac{Nu_2(x)}{\sqrt{Re_2(x)}} = 0.538 \left[\frac{3}{4} (m+1) f_w''(m) \right]^{1/3} Pr^{1/3} nx^{-n+\frac{m+1}{4}} J_2(x) = Pr^{1/3} B_2(m,n), \quad (42)$$

where $B_2(m,n)$ is independent of x . The function J_2 can be evaluated analytically in closed form for special pairs of values of m and n ; e.g., by use of the function $f_w''(m)$ in Fig. 2, $B_2(3,3) = 1.316$.

Both the low and the high Prandtl number methods and the exact solution for any Prandtl number yield expressions for $Nu_2(x)/\sqrt{Re_2(x)}$ which are independent of x as the comparison of equations (21), (25), (29), (39), and (42) shows. The functions $Nu_2(x)/\sqrt{Re_2(x)}$ are represented in Fig. 3 versus m for $n = 0$ and $Pr = 0.7$. The three methods, therefore, yield identical results for $Nu_2(x)/Nu_2(x^*)$, where x^* is any reference value.

VI. THE FUNCTIONS $u_e(x)$ AND $c_f(x)$ FOR THE INVESTIGATED CASES

Incompressible potential theory yields the velocity distribution

$$u_e(\varphi) = 2u_\infty \sin \varphi \quad (43)$$

at the surface of the circular cylinder presented in Fig. 5. In the vicinity of the stagnation point of this cylinder, $u_e(x_0) = 4u_\infty x_0/L$, where the coordinate x_0 measures along the circumference of the circular cross section, which possesses the diameter $L = 2R$. The velocity gradient $c = du_e(0)/dx$, then has the value $c = 4$. Also, according to reference 8, the velocity distribution

$$\frac{u_e(x)}{u_\infty} = 3.6314 \frac{x}{L} - 2.1709 \left(\frac{x}{L}\right)^3 - 1.5144 \left(\frac{x}{L}\right)^5 + \dots \quad \text{with } c = 3.6314 \quad (44)$$

follows from the measured pressure distribution around a circular cylinder in an airstream with the Reynolds number 19,000.

The functions

$$\xi_1 = a_1 \cos \varphi \quad \text{and} \quad \eta_1 = b_1 \sin \varphi \quad \text{with} \quad a_1 = R \left(1 + \frac{a^2}{R^2}\right), \quad b_1 = R \left(1 - \frac{a^2}{R^2}\right), \quad (45)$$

and $0 \leq a \leq R$ represent the conformal mapping of the $\xi_1 - \eta_1$ plane, Fig. 6, on the $\xi_0 - \eta_0$ plane, Fig. 5. The corresponding relation between the complex stream functions in the $\xi_1 - \eta_1$ plane and in the $\xi_0 - \eta_0$ plane is derived, e.g., on p. 121 of reference 18 and yields

$$\frac{u_e(\varphi(x))}{u_\infty} = \frac{1+\lambda}{\sqrt{1+\lambda^2 \operatorname{ctg}^2 \varphi}}, \quad \text{where } \lambda = \frac{b_1}{a_1}. \quad (46)$$

In a vicinity of the stagnation point $x = \varphi = 0$,

$$\frac{u_e(\varphi)}{u_\infty} = \frac{1+\lambda}{\lambda} \varphi = \frac{1+\lambda}{\lambda} \frac{x_0}{R} \quad \text{and} \quad \frac{x_0}{R} = \frac{1+\lambda}{2\lambda} \frac{x_1}{R} = \frac{1+\lambda}{2\lambda} \frac{x_1}{a_1} \left(1 + \frac{1-\lambda}{1+\lambda}\right) = \frac{1}{\lambda} \frac{x_1}{a_1}, \quad (47)$$

because of $a^2/R^2 = (1-\lambda)/(1+\lambda)$. Equation (47) yields

$$\frac{u_e(x_1)}{u_\infty} = 2 \frac{1+\lambda}{\lambda^2} \frac{x_1}{L} \quad \text{for } x_1 \ll 1, \quad (48)$$

where $L = 2a_1$. The functions (43) and (44) for the circular cross section and the function (46) for several elliptic cross sections are presented in Fig. 7.

Fig. 8, which represents data taken from reference 4, shows the surface velocity distribution $u_e(x)/u_\infty$ in planar incompressible flow for a single airfoil, $t/L = \infty$, and for the same airfoil in a cascade with $t/L = 0.5$.

The expression

$$c_f(x)\sqrt{\text{Re}_1} \equiv \frac{\tau_w(x)}{\frac{\rho}{2} u_\infty^2} \sqrt{\text{Re}_1} = 9.861 \frac{x}{L} - 3.863 \left(\frac{x}{L}\right)^3 + 0.413 \left(\frac{x}{L}\right)^5 - \dots \quad (49)$$

for the wall friction coefficient is, according to p. 136 of reference 19, a result of a series expansion of the solution for the laminar incompressible boundary layer around a circular cylinder. Fig. 9 presents $c_f(x)\sqrt{\text{Re}_1}$ versus x/L as following from the equation (37) for a flat plate with $m = 0$, from equation (49) for the circular cylinder, and from results of Kármán-Pohlhausen analyses, presented on p. 217 of reference 19 for the ellipses with the ratios 1:2 and 1:4 of the minor and major axes.

VII. DISCUSSION OF THE RESULTS

The heat flux equation

$$q_w(x) \equiv -k \frac{\partial T(x,0)}{\partial y} = \rho g c_p \frac{d}{dx} \int_0^{y_e} u(x,y) [T(x,y) - T_0] dy \quad (50)$$

of the temperature boundary layer is obtained by integration of the energy equation (3) across the boundary layer from $y = 0$ to the outer edge $y \approx y_e$. Since the temperature profile $T(x,y) - T_0$ cannot possess a point of inflection in problems of convective heat transfer with negligible frictional heating, equation (43) shows that the wall heat transfer rate $q_w(x)$ increases together with the level, in the vicinity of the wall, of the velocity component $u(x,y)$.

If a heat transfer problem of the type being considered with $0 < \text{Pr} < \infty$ is treated by use of the low Prandtl number method, $\text{Pr} \rightarrow 0$, $u(x,y)$ is replaced by $u_e(x)$, where $u(x,y) \leq u_e(x)$. The error of the low Prandtl number method, therefore, is positive and in general increases together with the boundary layer thickness, i.e., with x . The error then should take a minimum value at the forward stagnation point $x = 0$.

If a heat transfer problem with $0 < \text{Pr} < \infty$ is treated by use of the high Prandtl number method, $\text{Pr} \rightarrow \infty$, $u(x,y)$ is replaced by its wall tangent $y\tau_w(x)/\mu$. The error of the high Prandtl number method, therefore, is positive between the forward stagnation point $x = 0$ and a point close to the point $x = x_m$ of minimum pressure; the error is negative in the range $x_m < x < x_s$, where x_s is the point of separation of the boundary layer, since $u(x,y)$ as a function of y has a point of inflection for $x \geq x_m$. Fig. 4 shows for a flow with zero pressure gradient that the high Prandtl number method still yields the correct order of magnitude of $\text{Nu}_2(x)/\sqrt{\text{Re}_1(x)}$ for $\text{Pr} < 0.03$.

The x -independent relationship (15) between Nu_1 and $q_w(x)$ in case of constant wall temperature T_w shows that these conclusions on the deviations of the low and the high Prandtl number methods from exact solutions are valid for $\text{Nu}_1(x)$ as well as for $q_w(x)$. Therefore, the low Prandtl number method overestimates both $\text{Nu}_1(x)/\sqrt{\text{Re}_1}$ and $\text{Nu}_1(x)/\text{Nu}_1(0)$ at rates which increase together with x . The high Prandtl

number method overestimates $Nu_1(x)/\sqrt{Re_1}$ in the range $0 \leq x < x_m$ and underestimates $Nu_1(x)/\sqrt{Re_1}$ for $x > x_m$. The comparison of the two methods under discussion to exact similarity solutions in Fig. 3 confirms these conclusions. In particular, the error of the high Prandtl number method has different signs for $m > 0$ and for $m < 0$.

If the inevitable small inaccuracies of the quoted and of the calculated results are taken into account, Figures 10 through 15 confirm for constant wall temperature that the low Prandtl number method overestimates $Nu_1(x)/Nu_1(0)$ at a rate which increases together with x . The presented examples show that the high Prandtl number method underestimates $Nu_1(x)/Nu_1(0)$ for $0 \leq x < x_m$ in case of slender bodies. These conclusions still are valid between $x = 0$ and the point $x = \xi$ defined by $T_w(\xi) = T_0$ in case of variable wall temperature $T_w(x)$ (Figures 16 - 18).

The presented results, in particular the comparison of Figures 10 and 19 or 13 and 20, show for both the low and the high Prandtl number methods that the deviations of Nu/\sqrt{Re} from pertinent exact or approximate solutions can be represented as the products of large x -independent contributions, inherent to the methods, and of small x -dependent modifications, where only the latter part remains in $Nu(x)/Nu(0)$. This explains why it is advantageous to employ the result $Nu(x)/Nu(0)$ of the low or the high Prandtl number methods rather than their result $Nu(x)/\sqrt{Re}$.

If $T_w(x) = \text{const.}$ in a small vicinity of the forward stagnation point $x = 0$, the evaluation for $m = 1$ and $n = 0$ of the exact similarity solutions, e.g., equation (21), furnishes exact expressions for $Nu_1(0)/\sqrt{Re_1}$, which depend correctly on Pr . The product of the exact factor $Nu_1(0)/\sqrt{Re_1}$ and of the results $Nu_1(x)/Nu_1(0)$ of the low or the high Prandtl number methods yields satisfactory approximations to the exact solution for $Nu_1(x)/\sqrt{Re_1}$, and this in the total range of Prandtl numbers.

A comparison of equations (18) and (36) shows that the numerical evaluation of the high Prandtl number method is more involved than the one of the low Prandtl number method, in particular, if $T_w(x)$ is variable. Also, the input function $u_e(x)$ of the low Prandtl number method follows from ideal fluid flow theory, whereas the high Prandtl number method depends on the wall friction coefficient $c_f(x)$, which is a result of boundary layer analysis.

VIII. CONCLUSIONS

Both the low and the high Prandtl number methods yield closed form solutions for the wall heat transfer in the two limiting cases $Pr \rightarrow 0$, achieved through $\mu \rightarrow 0$, and $Pr \rightarrow \infty$, respectively. The error is investigated which is due to replacing a given heat transfer problem with $0 < Pr < \infty$ by the limiting problems. The results for $Nu_1(x)/Nu_1(0)$ of the low or the high Prandtl number methods yield significantly closer

$$c_f(x)\sqrt{Re_1} = \frac{\tau_w(x)}{\frac{\rho}{2} u_\infty^2} \sqrt{Re_1} = 9.861 \frac{x}{L} - 3.863 \left(\frac{x}{L}\right)^3 + 0.413 \left(\frac{x}{L}\right)^5 - \dots \quad (49)$$

for the wall friction coefficient is, according to p. 136 of reference 19, a result of a series expansion of the solution for the laminar incompressible boundary layer around a circular cylinder. Fig. 9 presents $c_f(x)\sqrt{Re_1}$ versus x/L as following from the equation (37) for a flat plate with $m = 0$, from equation (49) for the circular cylinder, and from results of Kármán-Pohlhausen analyses, presented on p. 217 of reference 19 for the ellipses with the ratios 1:2 and 1:4 of the minor and major axes.

VII. DISCUSSION OF THE RESULTS

The heat flux equation

$$q_w(x) \equiv -k \frac{\partial T(x,0)}{\partial y} = \rho g c_p \frac{d}{dx} \int_0^{y_e} u(x,y) [T(x,y) - T_0] dy \quad (50)$$

of the temperature boundary layer is obtained by integration of the energy equation (3) across the boundary layer from $y = 0$ to the outer edge $y \approx y_e$. Since the temperature profile $T(x,y) - T_0$ cannot possess a point of inflection in problems of convective heat transfer with negligible frictional heating, equation (43) shows that the wall heat transfer rate $q_w(x)$ increases together with the level, in the vicinity of the wall, of the velocity component $u(x,y)$.

If a heat transfer problem of the type being considered with $0 < Pr < \infty$ is treated by use of the low Prandtl number method, $Pr \rightarrow 0$, $u(x,y)$ is replaced by $u_e(x)$, where $u(x,y) \leq u_e(x)$. The error of the low Prandtl number method, therefore, is positive and in general increases together with the boundary layer thickness, i.e., with x . The error then should take a minimum value at the forward stagnation point $x = 0$.

If a heat transfer problem with $0 < Pr < \infty$ is treated by use of the high Prandtl number method, $Pr \rightarrow \infty$, $u(x,y)$ is replaced by its wall tangent $y\tau_w(x)/\mu$. The error of the high Prandtl number method, therefore, is positive between the forward stagnation point $x = 0$ and a point close to the point $x = x_m$ of minimum pressure; the error is negative in the range $x_m < x < x_s$, where x_s is the point of separation of the boundary layer, since $u(x,y)$ as a function of y has a point of inflection for $x \geq x_m$. Fig. 4 shows for a flow with zero pressure gradient that the high Prandtl number method still yields the correct order of magnitude of $Nu_2(x)/\sqrt{Re(x)}$ for $Pr < 0.03$.

The x -independent relationship (15) between Nu_1 and $q_w(x)$ in case of constant wall temperature T_w shows that these conclusions on the deviations of the low and the high Prandtl number methods from exact solutions are valid for $Nu_1(x)$ as well as for $q_w(x)$. Therefore, the low Prandtl number method overestimates both $Nu_1(x)/\sqrt{Re_1}$ and $Nu_1(x)/Nu_1(0)$ at rates which increase together with x . The high Prandtl

number method overestimates $Nu_1(x)/\sqrt{Re_1}$ in the range $0 \leq x < x_m$ and underestimates $Nu_1(x)/\sqrt{Re_1}$ for $x > x_m$. The comparison of the two methods under discussion to exact similarity solutions in Fig. 3 confirms these conclusions. In particular, the error of the high Prandtl number method has different signs for $m > 0$ and for $m < 0$.

If the inevitable small inaccuracies of the quoted and of the calculated results are taken into account, Figures 10 through 15 confirm for constant wall temperature that the low Prandtl number method overestimates $Nu_1(x)/Nu_1(0)$ at a rate which increases together with x . The presented examples show that the high Prandtl number method underestimates $Nu_1(x)/Nu_1(0)$ for $0 \leq x < x_m$ in case of slender bodies. These conclusions still are valid between $x = 0$ and the point $x = \xi$ defined by $T_w(\xi) = T_0$ in case of variable wall temperature $T_w(x)$ (Figures 16 - 18).

The presented results, in particular the comparison of Figures 10 and 19 or 13 and 20, show for both the low and the high Prandtl number methods that the deviations of Nu/\sqrt{Re} from pertinent exact or approximate solutions can be represented as the products of large x -independent contributions, inherent to the methods, and of small x -dependent modifications, where only the latter part remains in $Nu(x)/Nu(0)$. This explains why it is advantageous to employ the result $Nu(x)/Nu(0)$ of the low or the high Prandtl number methods rather than their result $Nu(x)/\sqrt{Re}$.

If $T_w(x) = \text{const.}$ in a small vicinity of the forward stagnation point $x = 0$, the evaluation for $m = 1$ and $n = 0$ of the exact similarity solutions, e.g., equation (21), furnishes exact expressions for $Nu_1(0)/\sqrt{Re_1}$, which depend correctly on Pr . The product of the exact factor $Nu_1(0)/\sqrt{Re_1}$ and of the results $Nu_1(x)/Nu_1(0)$ of the low or the high Prandtl number methods yields satisfactory approximations to the exact solution for $Nu_1(x)/\sqrt{Re_1}$, and this in the total range of Prandtl numbers.

A comparison of equations (18) and (36) shows that the numerical evaluation of the high Prandtl number method is more involved than the one of the low Prandtl number method, in particular, if $T_w(x)$ is variable. Also, the input function $u_e(x)$ of the low Prandtl number method follows from ideal fluid flow theory, whereas the high Prandtl number method depends on the wall friction coefficient $c_f(x)$, which is a result of boundary layer analysis.

VIII. CONCLUSIONS

Both the low and the high Prandtl number methods yield closed form solutions for the wall heat transfer in the two limiting cases $Pr \rightarrow 0$, achieved through $\mu \rightarrow 0$, and $Pr \rightarrow \infty$, respectively. The error is investigated which is due to replacing a given heat transfer problem with $0 < Pr < \infty$ by the limiting problems. The results for $Nu_1(x)/Nu_1(0)$ of the low or the high Prandtl number methods yield significantly closer

approximations than their results for $Nu_1(x)/\sqrt{Re_1}$. The expressions $Nu_2(x)/Nu_2(x^*)$ as obtained from the low and the high Prandtl number methods and from exact boundary layer solutions coincide in the similarity case defined by the power laws (19) for $u_e(x)$ and $T_w(x) - T_0$. It is shown theoretically and confirmed by the numerical results that the low Prandtl number method yields an upper limit for both $Nu_1(x)/\sqrt{Re_1}$ and $Nu_1(x)/Nu_1(0)$. Theoretical conclusions and the presented data yield the result that the high Prandtl number method overestimates $Nu_1(x)/\sqrt{Re_1}$ in the region of accelerated flow and underestimates $Nu_1(x)/\sqrt{Re_1}$ in the region of decelerated flow. The presented examples show for slender bodies that the high Prandtl number method furnishes a lower limit for $Nu_1(x)/Nu_1(0)$ in the region of accelerated flow. Since exact solutions for $Nu_1(0)/\sqrt{Re_1}$ exist at the stagnation point $x = 0$ for a very wide range of Prandtl numbers, if the temperature $T_w = \text{const.}$ in a small vicinity of the stagnation point, the product of the exact factor $Nu_1(0)/\sqrt{Re_1}$ and of the results $Nu_1(x)/Nu_1(0)$ of the low or the high Prandtl number methods, respectively, yields satisfactory approximations for $Nu_1(x)/\sqrt{Re_1}$ in the range $0 \leq Pr \leq \infty$. The amount of work involved in calculating the input function $u_e(x)$ and in evaluating the low Prandtl number method is significantly smaller than the amount of work involved in solving the boundary layer equations for the input function $c_f(x)\sqrt{Re_1}$ and in evaluating the high Prandtl number method.

APPENDIX

THE SOLUTION OF THE EQUATIONS (7) - (10)

The differential equation (7) together with the initial and boundary conditions (8) - (10) can be solved by the expression

$$T(\varnothing, \psi) - T_0 = \int_{\eta=0}^{\eta=\varnothing} [T_w(\eta) - T_0] \frac{\partial}{\partial \varnothing} F(\varnothing - \eta, \psi) d\eta, \quad (\text{A-1})$$

according to p. 62 of reference 1, where η is a dummy variable for \varnothing in the limits $0 \leq \eta \leq \varnothing$. The function

$$F(\varnothing - \eta, \psi) = \frac{2}{\sqrt{\pi}} \int_{\frac{\psi}{2\sqrt{A(\varnothing - \eta)}}}^{\infty} e^{-\eta^2} d\eta \quad \text{with } A = \frac{k}{\rho g c_p} \quad (\text{A-2})$$

is related to the error integral $\text{erf}_x = \frac{2}{\sqrt{\pi}} \int_0^x e^{-\xi^2} d\xi$. Both $F(\varnothing - \eta, \psi)$

and its derivatives are well defined for $\eta < \varnothing$ and their limits exist as $\eta \rightarrow \varnothing$ for $\psi > 0$; at the point $\psi = 0$ and $\eta = \varnothing$, however, these functions do not possess unique limits. The equations (A-1) and (A-2) yield the relation

$$T(\varnothing, \psi) - T_0 = \frac{\psi}{2\sqrt{A\pi}} \int_{\eta=0}^{\eta=\varnothing} [T_w(\eta) - T_0] \frac{\exp[-\psi^2/4A(\varnothing - \eta)]}{(\varnothing - \eta)^{3/2}} d\eta \quad \text{for } \psi > 0. \quad (\text{A-3})$$

It is immediately seen that the relation (A-3) satisfies the conditions (8) and (10). Since the derivatives of (A-3) exist for $\psi > 0$, it can be shown for $\psi > 0$ that the relation (A-3) satisfies the differential equation (7). It is shown in the following paragraph that the relation (A-3) satisfies the remaining boundary condition (9).

Equation (A-3) becomes

$$T(\varnothing, \psi) - T_0 = \frac{2}{\sqrt{\pi}} \int_{\mu = \frac{\psi}{2\sqrt{A\varnothing}}}^{\infty} [T_w(\varnothing - \psi^2/4A\mu^2) - T_0] e^{-\mu^2} d\mu \quad (\text{A-4})$$

when the coordinate transformation

$$\mu = \frac{\psi}{2\sqrt{A(\varnothing-\eta)}} \quad (\text{A-5})$$

is introduced, which relates the independent variables η and μ and which exists if $\varnothing > 0$ and $\psi > 0$. The integrand in equation (A-4) possesses the following finite discontinuity at the point defined by $\mu = 0$ and $\psi = 0$:

$$\lim_{\psi \rightarrow 0} T_w\left(\varnothing - \frac{\psi^2}{4A\mu^2}\right) - T_0 = \begin{cases} T_w(\varnothing) - T_0 & \text{for } \mu > \frac{\psi}{2\sqrt{A\varnothing}} \text{ and } \varnothing > 0 \\ T_w(0) - T_0 = 0 < T_w(\varnothing) - T_0 & \text{for } \mu = \frac{\psi}{2\sqrt{A\varnothing}} \text{ and } \varnothing > 0 \end{cases} \quad (\text{A-6})$$

The integral in equation (A-4) can be expressed as the sum of the "main part" pertaining to the range $\epsilon + \frac{\psi}{2\sqrt{A\varnothing}} \leq \mu \leq \infty$, where $0 < \epsilon \ll 1$, and

of the "remainder" for the range $\frac{\psi}{2\sqrt{A\varnothing}} \leq \mu \leq \epsilon + \frac{\psi}{2\sqrt{A\varnothing}}$. If the integrand

in the remainder is replaced by its upper limit $T_w(\varnothing) - T_0$, according to the relations (A-6), it is seen for $\varnothing > 0$ that the resulting upper limit of the remainder tends to zero together with ϵ at any value of ψ . Because

of $\int_0^\infty e^{-\mu^2} d\mu = \sqrt{\pi}/2$, the main part then tends to the limit $T_w(\varnothing) - T_0$

when ϵ and ψ tend to zero independently of one another; i.e., the boundary condition (9) is satisfied by the relation (A-3).

The integration by parts is valid in the right-hand side of equation (A-3) since the integrals converge uniformly for $\psi > 0$ and $0 \leq \varnothing \leq \infty$. Because of $\partial F / \partial \varnothing = -\partial F / \partial \psi$ and $\lim_{\eta \rightarrow \varnothing} F(\varnothing - \eta, \psi) = 0$, equation (A-3) then becomes

$$T(\varnothing, \psi) - T_0 = \int_{\eta=0}^{\eta=\varnothing} \frac{dT_w(\eta)}{d\eta} F(\varnothing - \eta, \psi) d\eta \quad \text{for } \psi > 0 \text{ and } T_w(0) = T_0. \quad (\text{A-7})$$

Since equation (A-7) may be differentiated if $\psi > 0$,

$$\frac{\partial T(\varnothing, \psi)}{\partial \psi} = -\frac{2}{\sqrt{\pi}} \int_{\eta=0}^{\eta=\varnothing} \frac{dT_w(\eta)}{d\eta} \frac{\exp[-\psi^2/4A(\varnothing-\eta)]}{2\sqrt{A(\varnothing-\eta)}} d\eta \quad \text{for } \psi > 0 \text{ and } T_w(0) = T_0. \quad (\text{A-8})$$

The integrand in equation (A-8) possesses a finite discontinuity at the point defined by $\eta = \varnothing$ and $\psi = 0$. Because of $0 \leq \exp [\psi^2/4A(\varnothing-\eta)] < 1$, it can be shown by an argument following the one presented above that the limiting form of the equation as $\psi \rightarrow 0$ is

$$\frac{\partial T(\varnothing, 0)}{\partial \psi} = - \sqrt{\frac{\rho g c_p}{\pi k}} \int_{\eta=0}^{\eta=\varnothing} \frac{dT_w(\eta)}{d\eta} \frac{d\eta}{\sqrt{\varnothing-\eta}} \quad (A-9)$$

For constant wall temperature, $T_w(\varnothing) - T_o \equiv T_w(0) - T_o = \text{const.}$, equation (A-1) becomes because of $\partial F/\partial \varnothing = - \partial F/\partial \eta$

$$T(\varnothing, \psi) - T_o = -[T_w(0) - T_o] F(\varnothing - \eta, \psi) \Big|_{\eta=0}^{\eta=\varnothing} = \frac{2}{\sqrt{\pi}} [T_w(0) - T_o] \int_{\psi/2\sqrt{A\varnothing}}^{\infty} e^{-\xi^2} d\xi \quad (A-10)$$

except at the point defined by $\varnothing = 0$ and $\psi = 0$. Equation (A-10) satisfies the initial and boundary conditions (8) - (10) because of

$$\int_0^{\infty} e^{-\xi^2} d\xi = \frac{\sqrt{\pi}}{2}. \quad \text{Also,}$$

$$\frac{\partial T(\varnothing, \psi)}{\partial \psi} = -\frac{2}{\sqrt{\pi}} [T_w(0) - T_o] \frac{\exp[-\psi^2/4A\varnothing]}{2\sqrt{A\varnothing}} \quad \text{and} \quad (A-11)$$

$$\frac{\partial T(\varnothing, 0)}{\partial \psi} = -\sqrt{\frac{\rho g c_p}{\pi k}} \frac{T_w(0) - T_o}{\sqrt{\varnothing}} \quad \text{for } \varnothing > 0. \quad (A-12)$$

Since the velocity distribution $u_e(x)$ prevails at the wall in the limit $\mu \rightarrow 0$ under discussion, equations (A-9) and (A-12) yield the following expression:

$$\frac{\partial T(x, 0)}{\partial y} = -\sqrt{\frac{\rho g c_p}{\pi k}} u_e(x) \left[\frac{T_w(0) - T_o}{\sqrt{\varnothing(x)}} + \int_{\eta=0}^{\eta=\varnothing(x)} \frac{dT_w(\eta)}{d\eta} \frac{d\eta}{\sqrt{\varnothing-\eta}} \right] \quad (A-13)$$

Non-dimensional wall temperature gradient $\left\{(-\sqrt{xL}/Re_1)(\partial T/\partial y)_w \left[1/(T_w - T_o)\right]\right\}$ versus Prandtl number Pr for flat plate at constant wall temperature T_w in uniform flow, data taken from Fig. 1 of Ref. 14.

Curve No. 1: Result of Kármán-Pohlhausen analysis, presented in Ref. 21

Curve No. 2: Low Prandtl number approach

Curve No. 3: Low Prandtl number approach plus correction term taken from Ref. 14

The points marked by \odot represent the exact solution in Ref. 16.

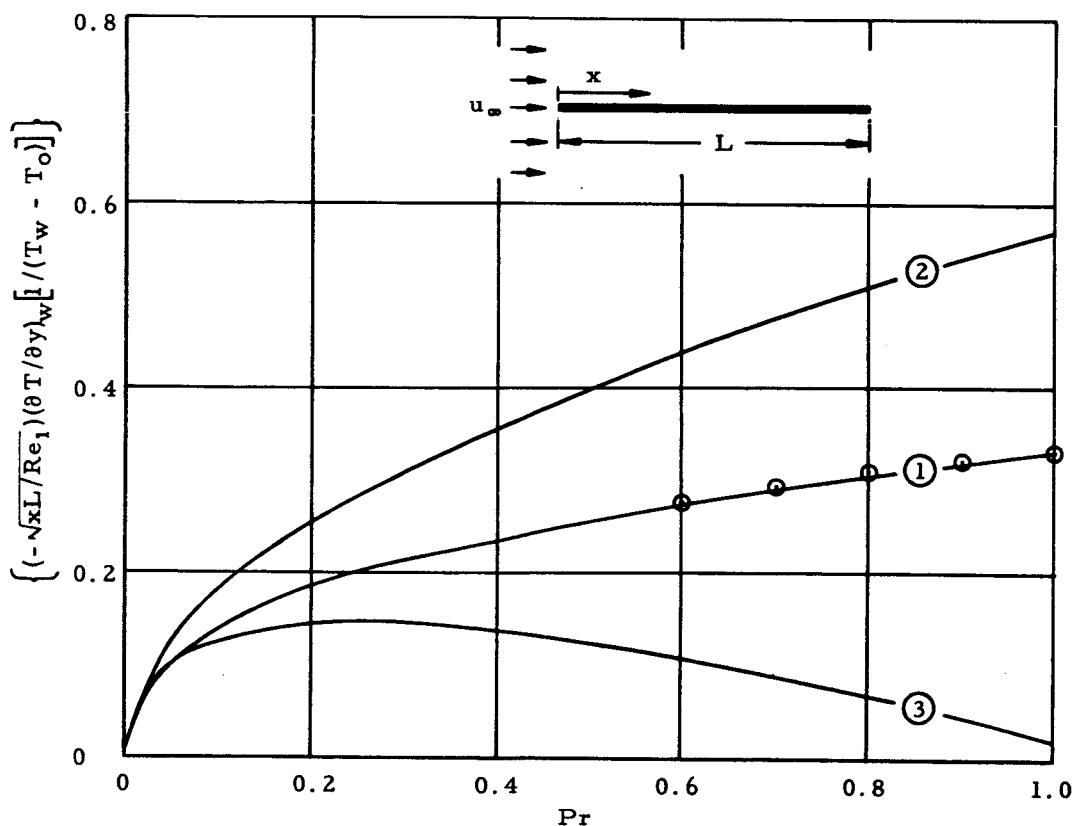


FIG. 1. NON-DIMENSIONAL WALL TEMPERATURE GRADIENT FOR FLAT PLATE

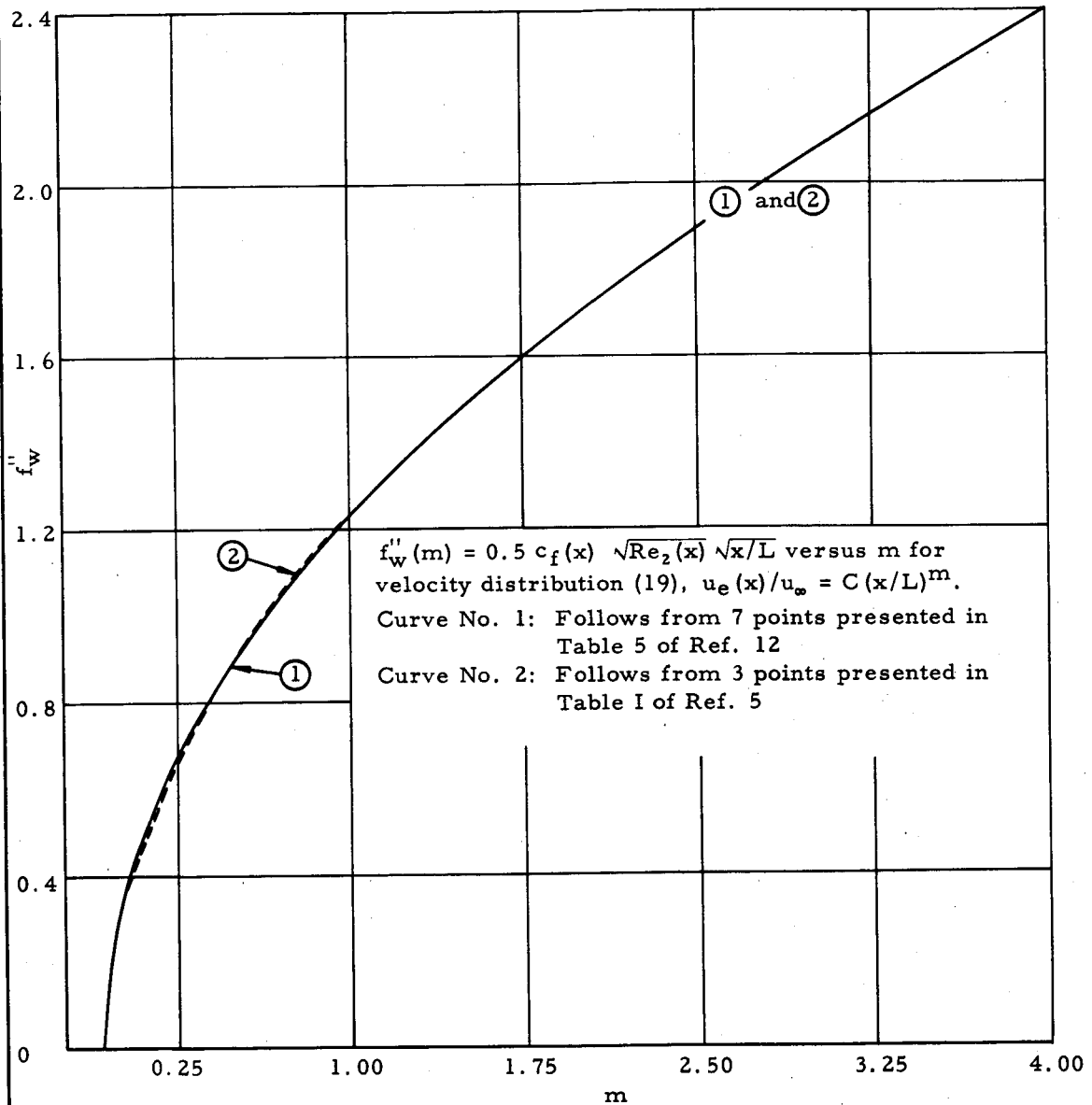


FIG. 2. NON-DIMENSIONAL FRICTION COEFFICIENT FROM EXACT SIMILARITY SOLUTIONS

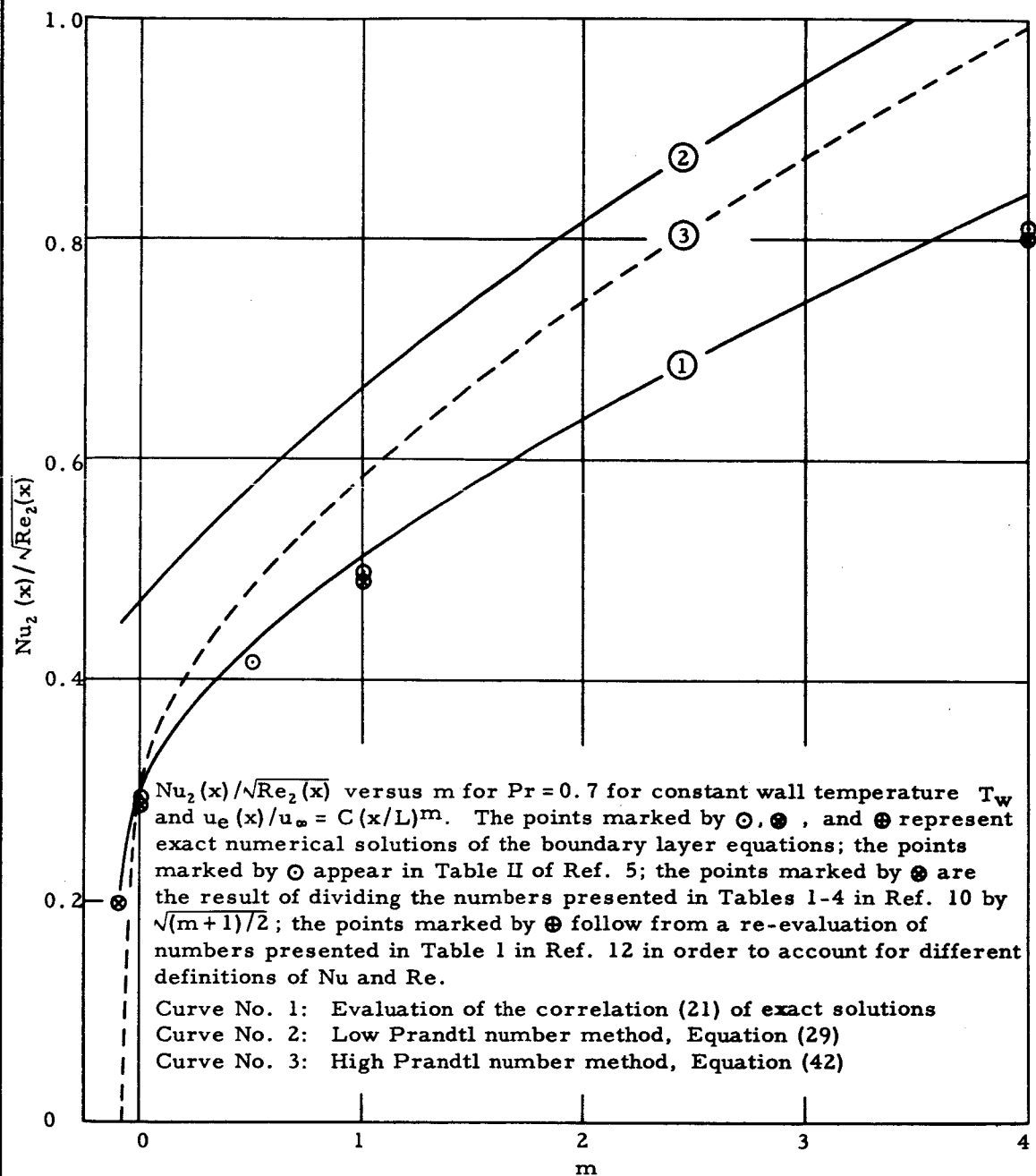


FIG. 3. $Nu_2(x)/\sqrt{Re_2(x)}$ FROM EXACT SIMILARITY SOLUTIONS

$Nu_2(x)/\sqrt{Re_2(x)Pr}$ versus Pr for a flat plate with $u_e(x) = u_\infty$ at constant wall temperature T_w .

Curve No. 1: Exact numerical solution derived in Ref. 22

Curve No. 2: Result of Kármán-Pohlhausen analysis in Ref. 21, yielding $Nu_2(x)/\sqrt{Re_2(x)Pr} = 0.529/(1 + 0.82\sqrt{Pr})$

Curve No. 3: Low Prandtl number approach, Equation (12)

Curve No. 4: Low Prandtl number approach plus correction term taken from Ref. 14, yielding $Nu_2(x)/\sqrt{Re_2(x)Pr} = 0.564 - 0.547\sqrt{Pr}$

Curve No. 5: High Prandtl number approach, Equation (32)

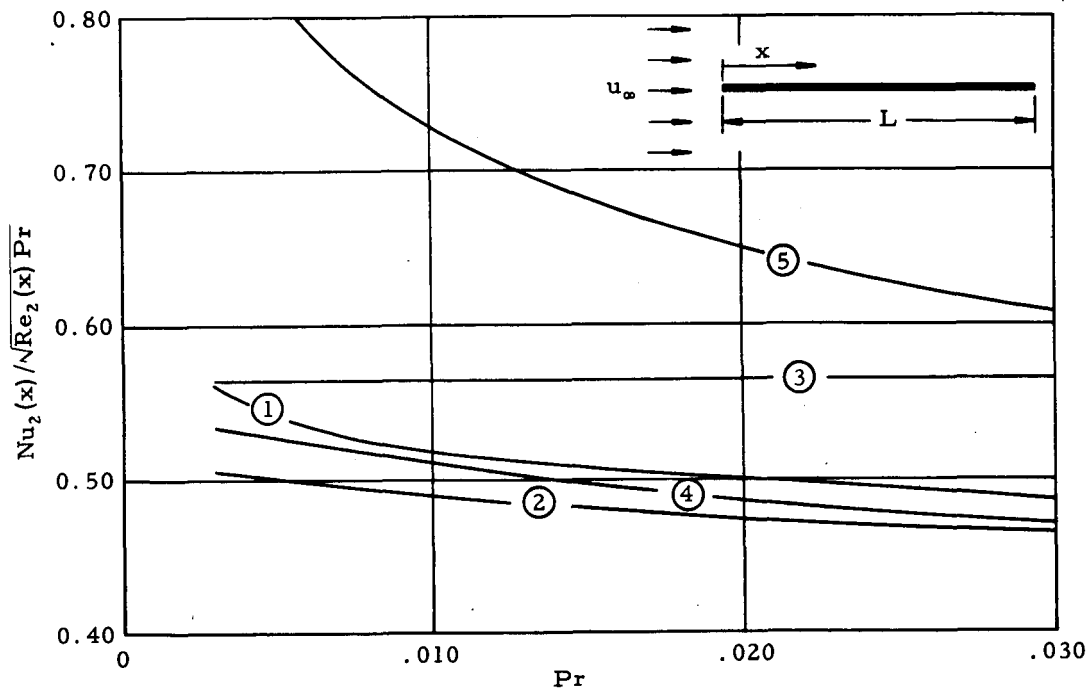


FIG. 4. $Nu_2(x)/\sqrt{Re_2(x)Pr}$ FOR FLAT PLATE

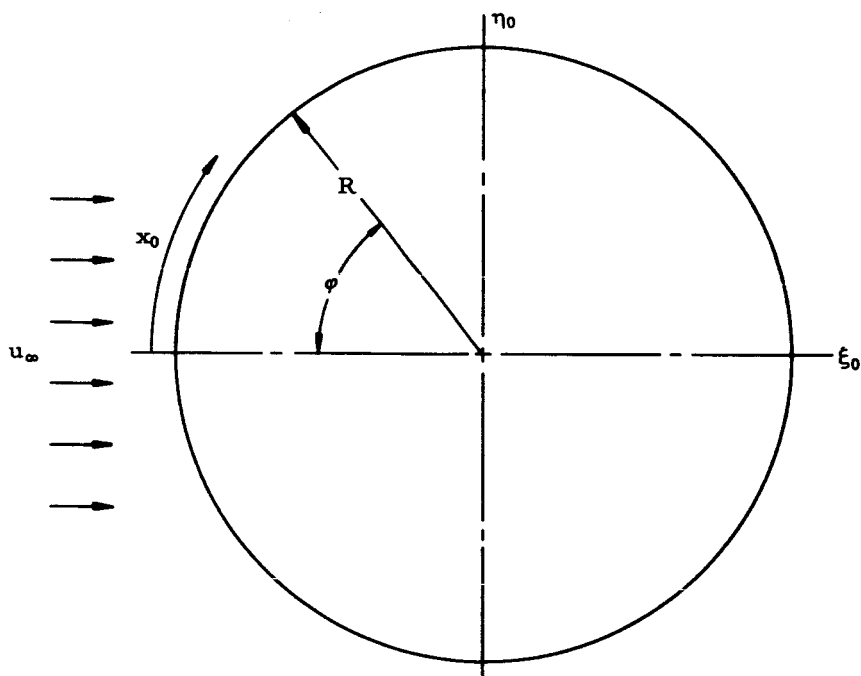


FIG. 5. CIRCULAR CYLINDER IN UNIFORM PLANAR FLOW IN THE ξ_0 - η_0 PLANE

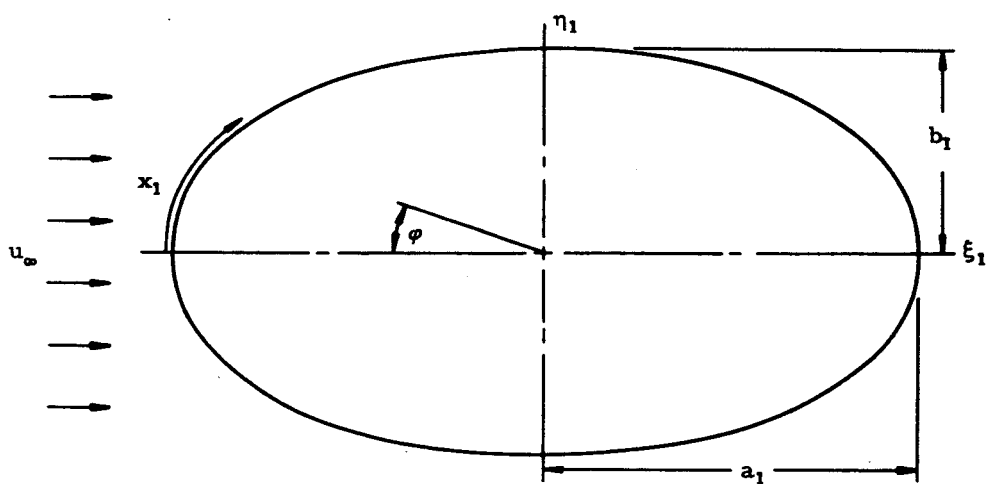


FIG. 6. ELLIPTICAL CYLINDER IN UNIFORM PLANAR FLOW IN THE ξ_1 - η_1 PLANE

$u_e(x)/u_\infty$ for several cylinders in uniform planar flow.

Curve No. 1: Evaluation of the Equation (43) for the circular cylinder, which follows from potential theory

Curve No. 2: Evaluation of the Equation (44) for the circular cylinder, which follows from measurements at $Re_1 = 19,000$, see Ref. 8

Curve No. 3: Evaluation of the Equation (46) for the elliptic cylinder with the ratio 1:2 of the axes

Curve No. 4: Evaluation of the Equation (46) for the elliptic cylinder with the ratio 1:4 of the axes

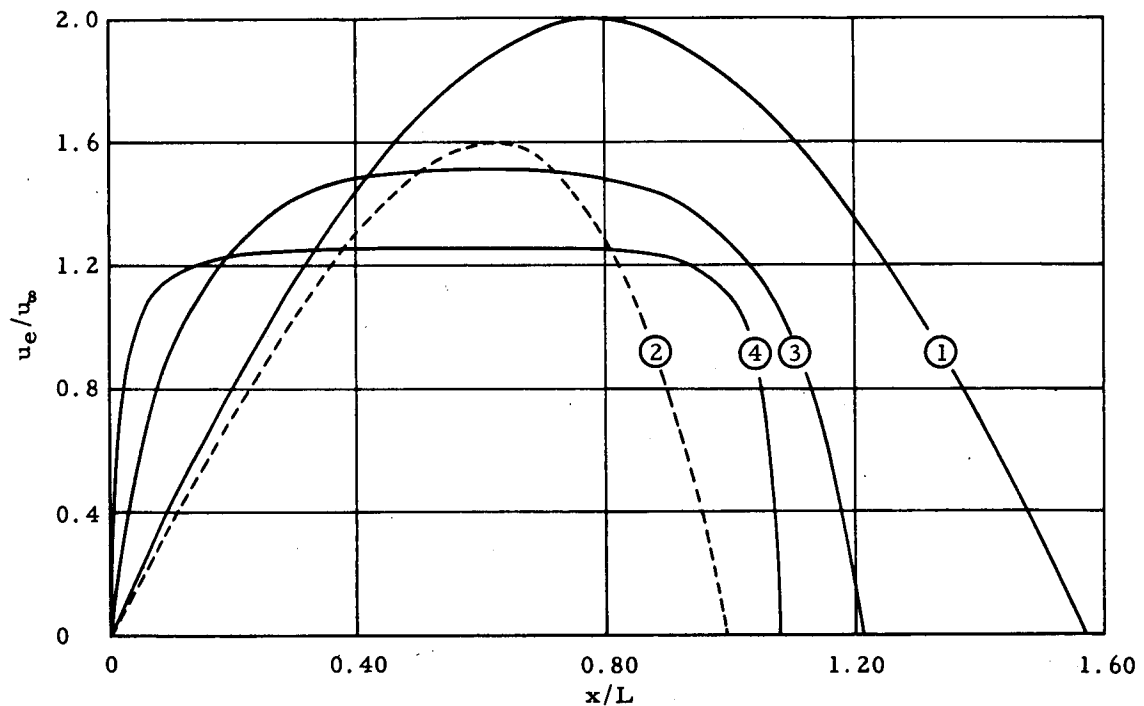


FIG. 7. VELOCITY DISTRIBUTIONS AT SURFACES OF CIRCULAR AND ELLIPTIC CYLINDERS

$u_e(x)/u_\infty$ versus x/L for airfoils in uniform planar flow, data taken from p. 98 of Ref. 4.

Curve No. 1: Single airfoil, $t/L = \infty$

Curve No. 2: Same airfoil in cascade flow with $t/L = 0.5$

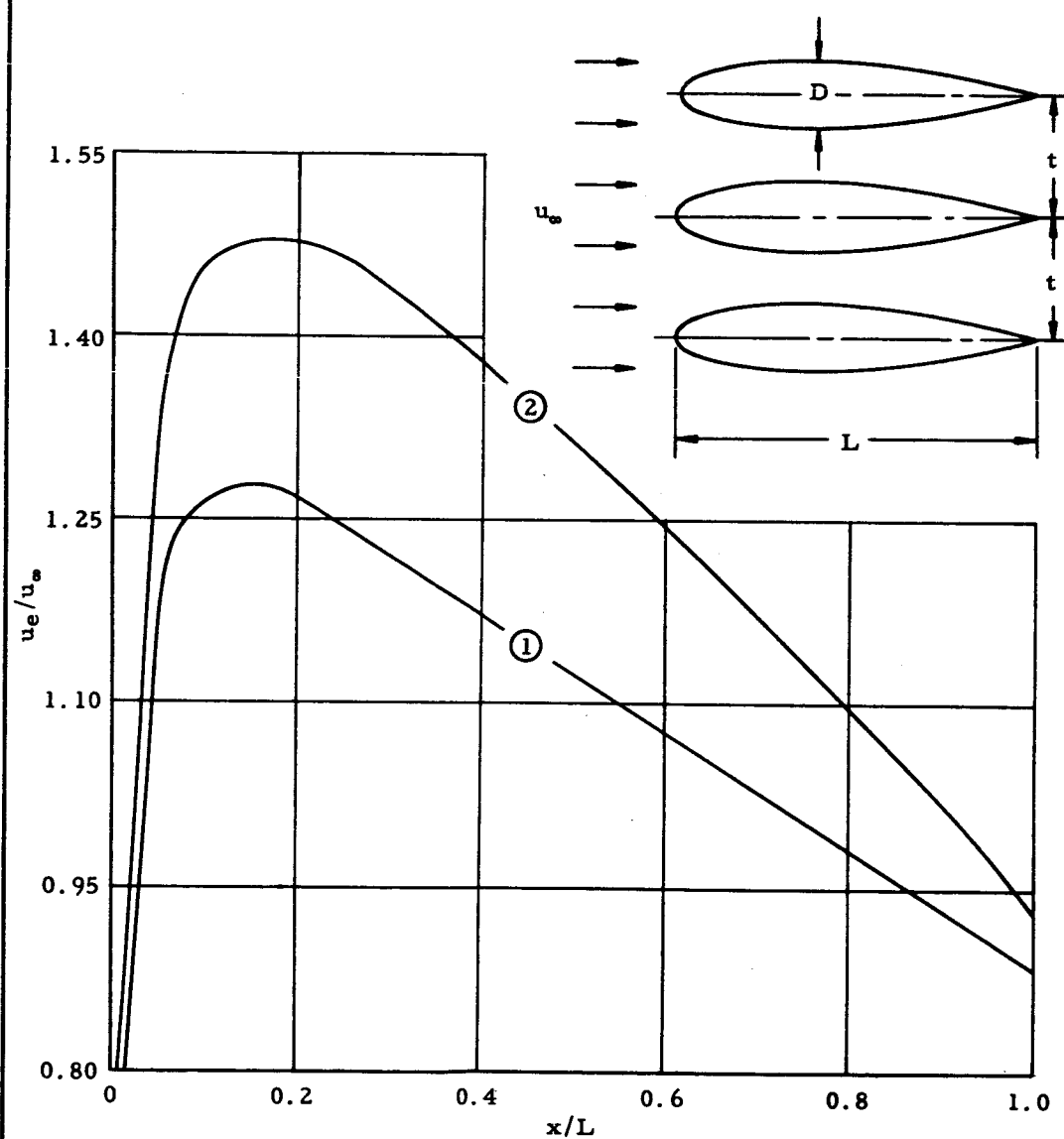


FIG. 8. VELOCITY DISTRIBUTIONS AT SURFACE OF AIRFOIL

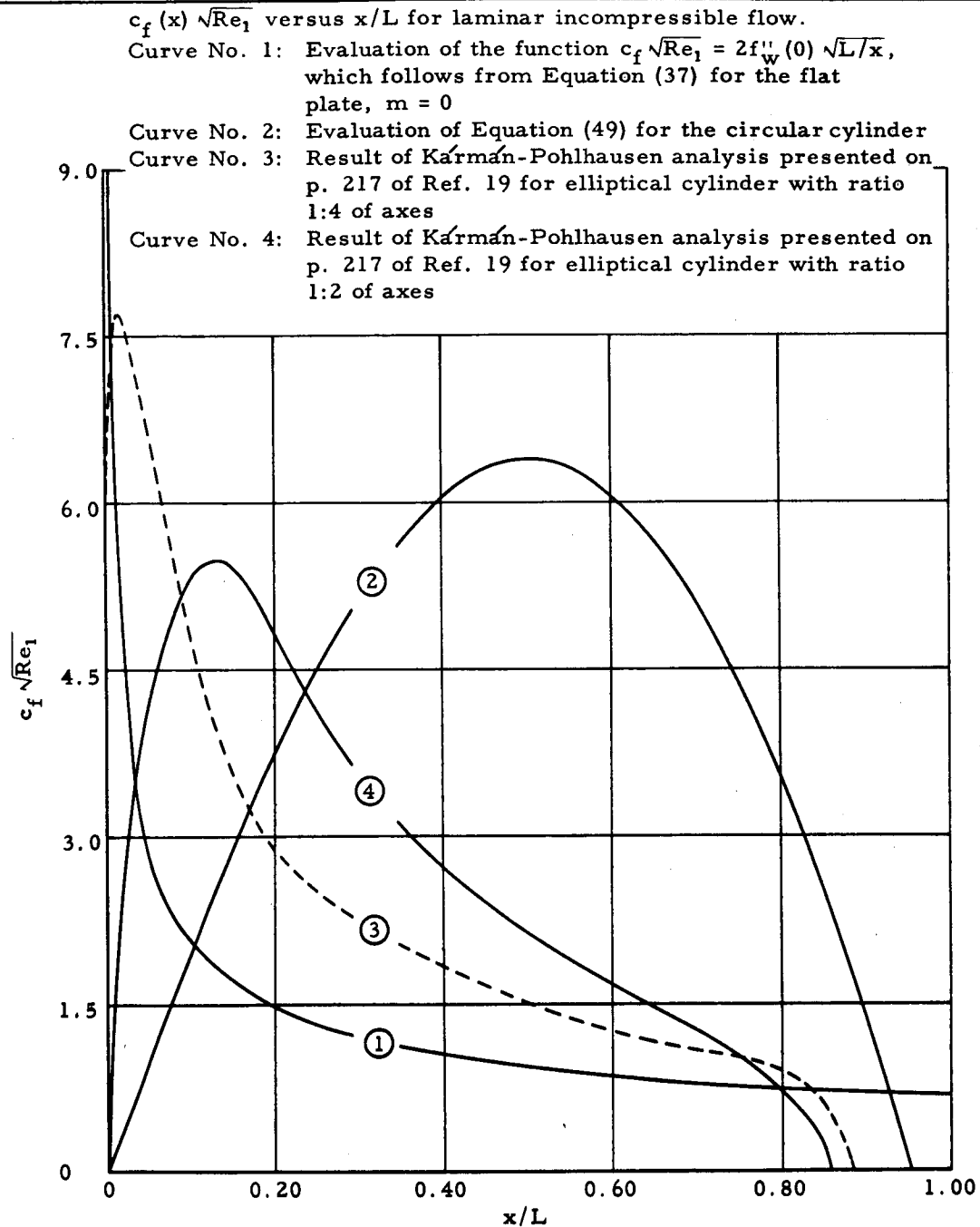


FIG. 9. FRICTION COEFFICIENT FOR FLAT PLATE, CIRCULAR, AND ELLIPTIC CYLINDER

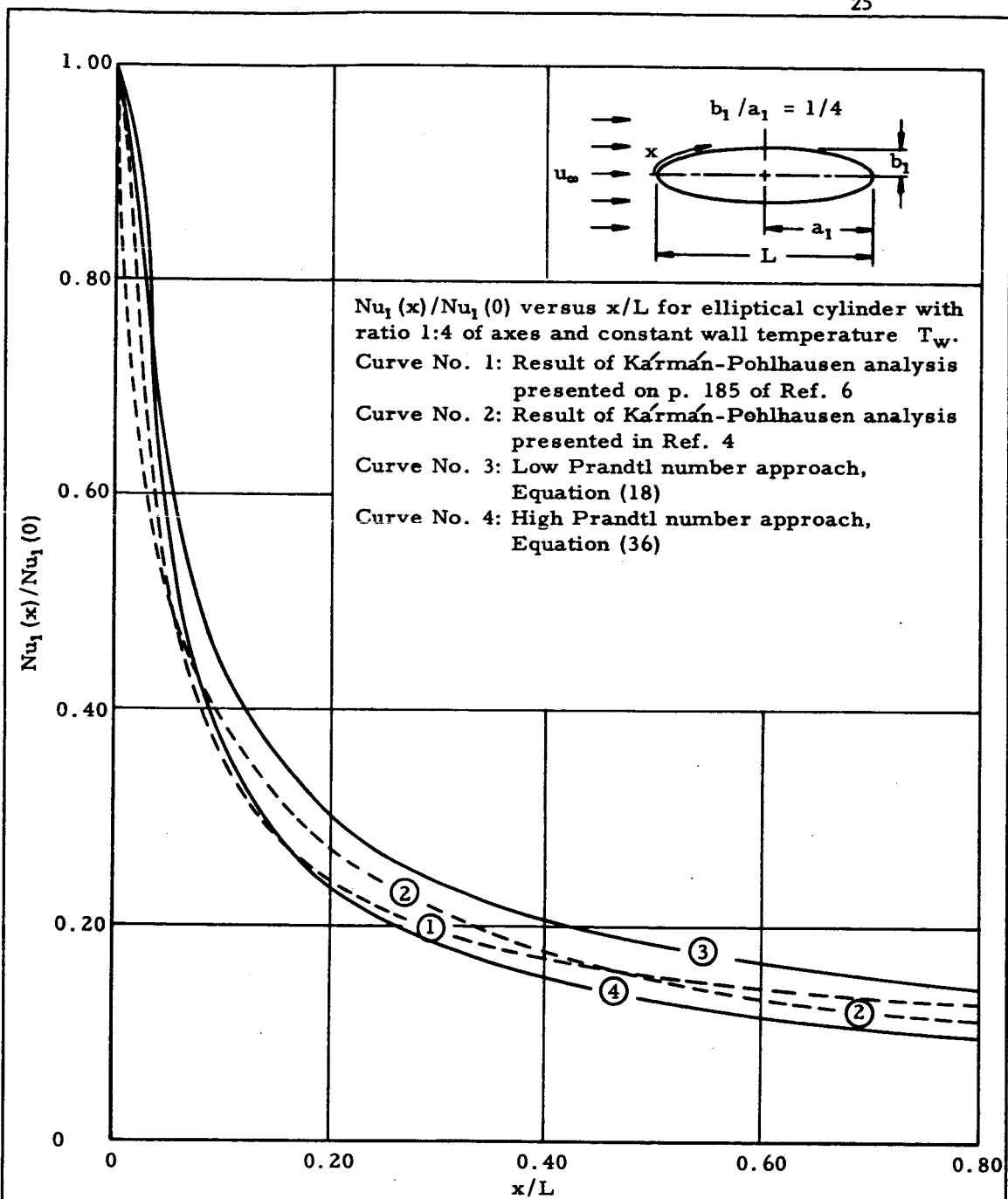


FIG. 10. $Nu_1(x)/Nu_1(0)$ FOR ELLIPTICAL CYLINDER 1:4,
 $T_w = \text{CONST.}$

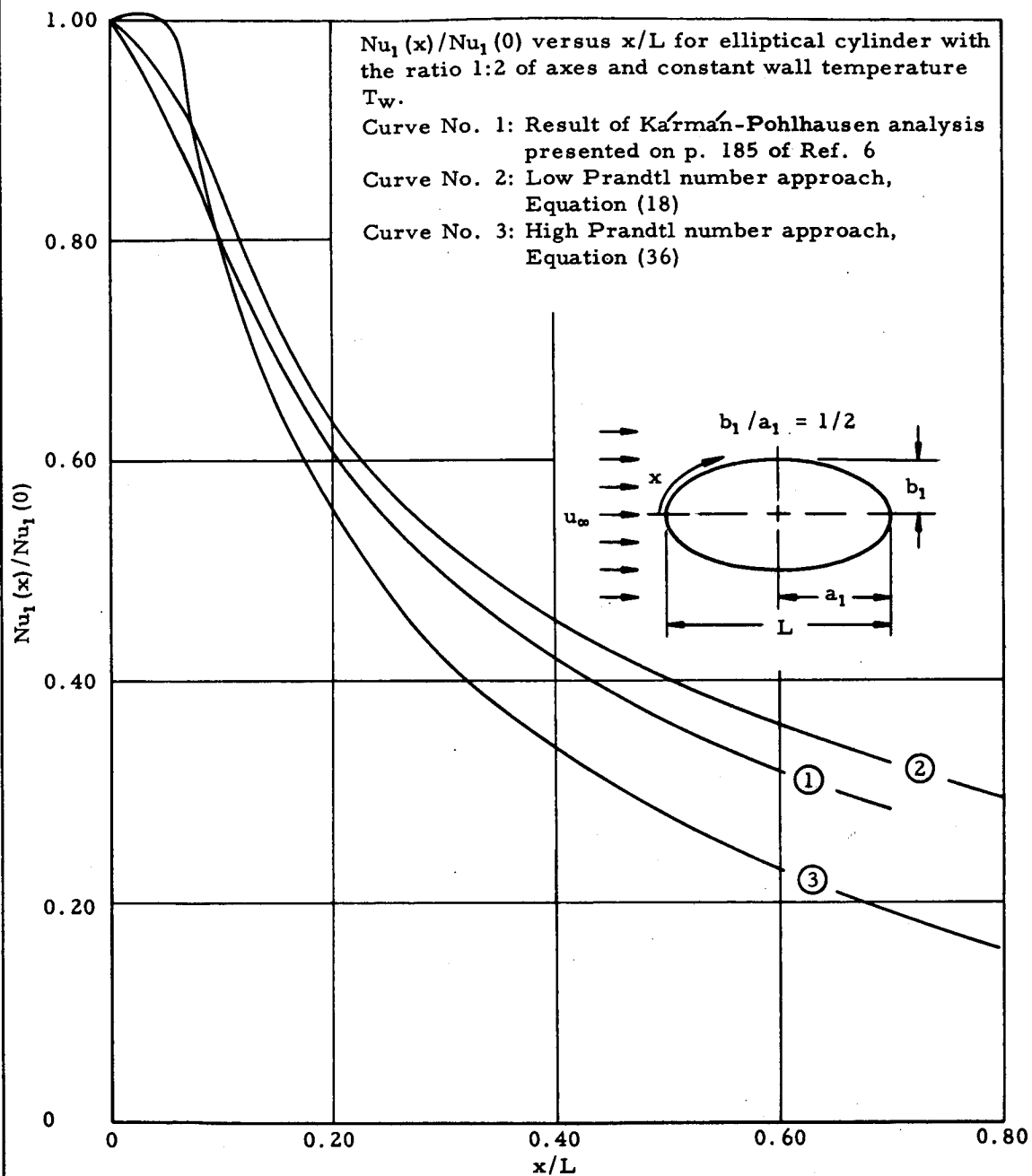


FIG. 11. $Nu_1(x)/Nu_1(0)$ FOR ELLIPTICAL CYLINDER 1:2,
 $T_w = \text{CONST.}$

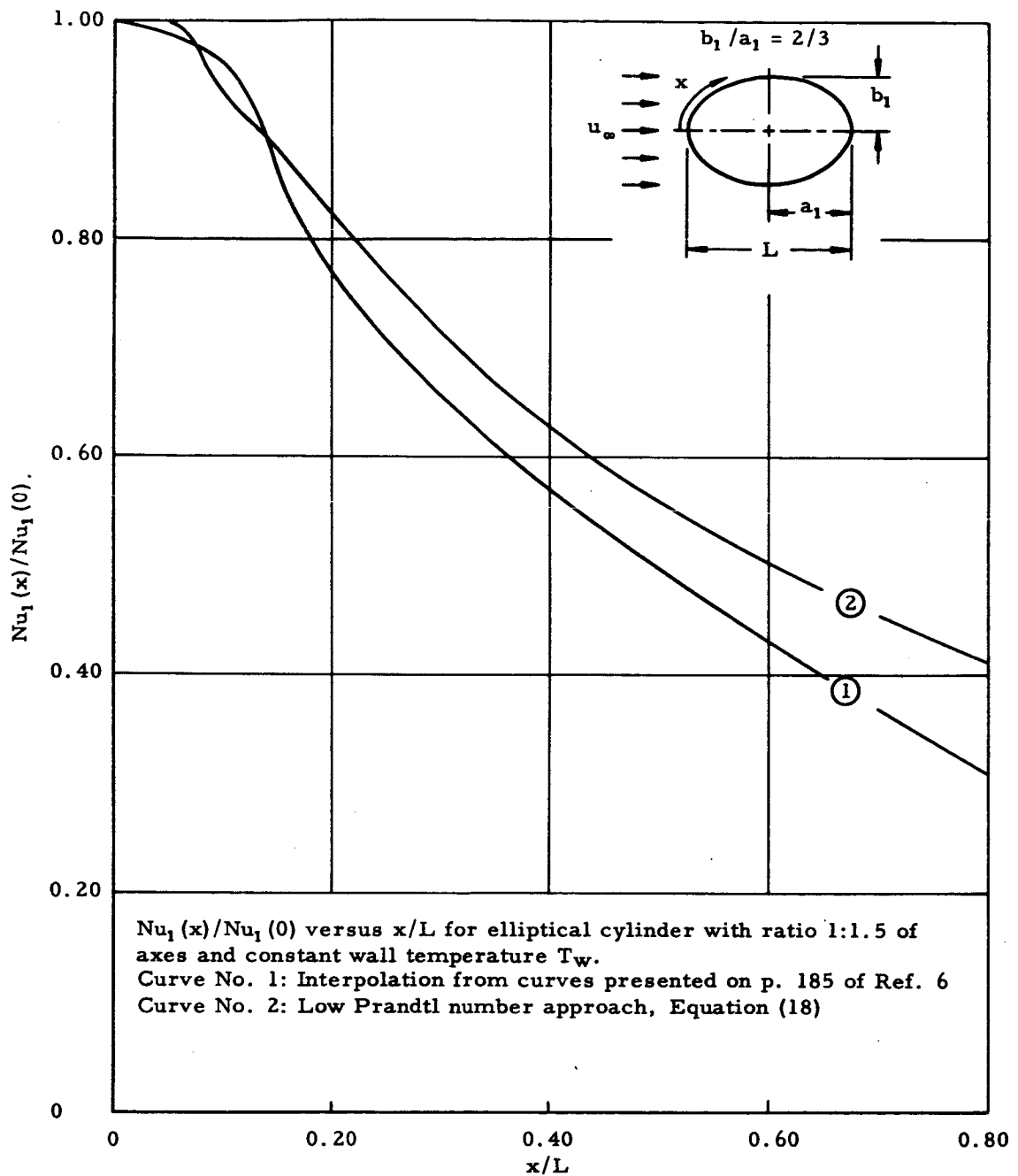


FIG. 12. $Nu_1(x)/Nu_1(0)$ FOR ELLIPTICAL CYLINDER 1:1.5, $T_w = \text{CONST.}$

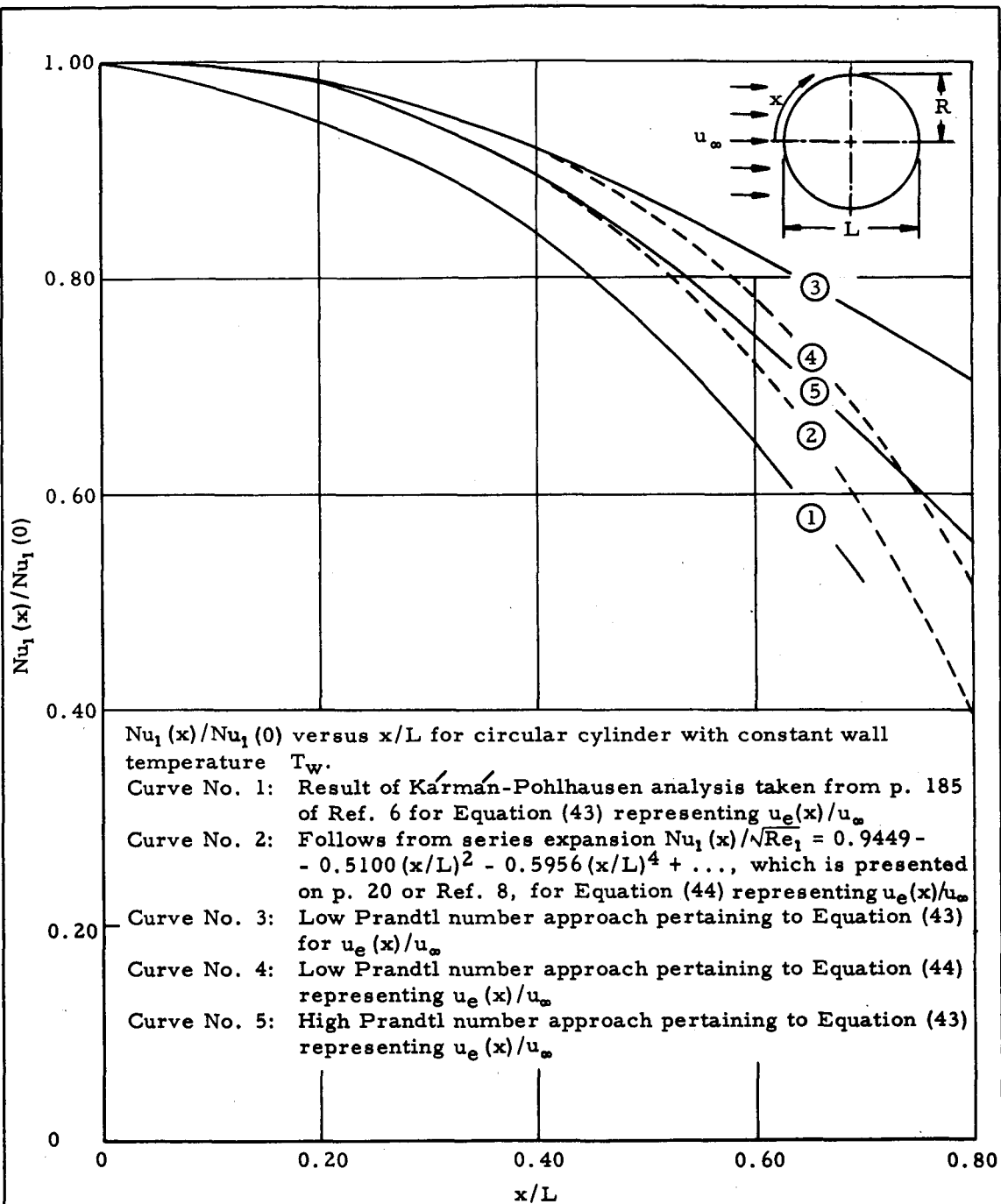


FIG. 13. $Nu_1(x)/Nu_1(0)$ FOR CIRCULAR CYLINDER,
 $T_w = \text{CONST.}$

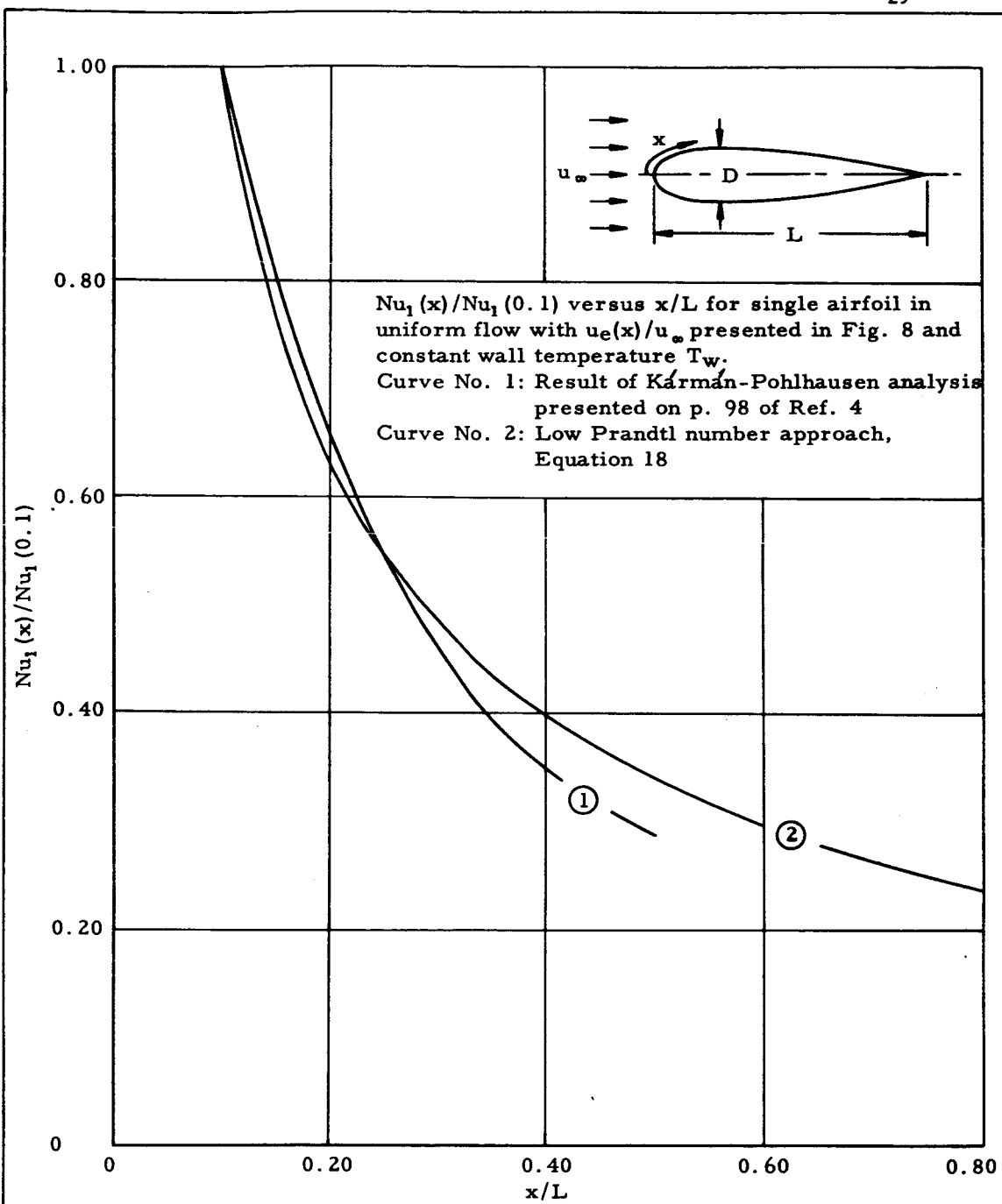


FIG. 14. $Nu_1(x)/Nu_1(0.1)$ FOR SINGLE AIRFOIL, $T_w = \text{CONST.}$

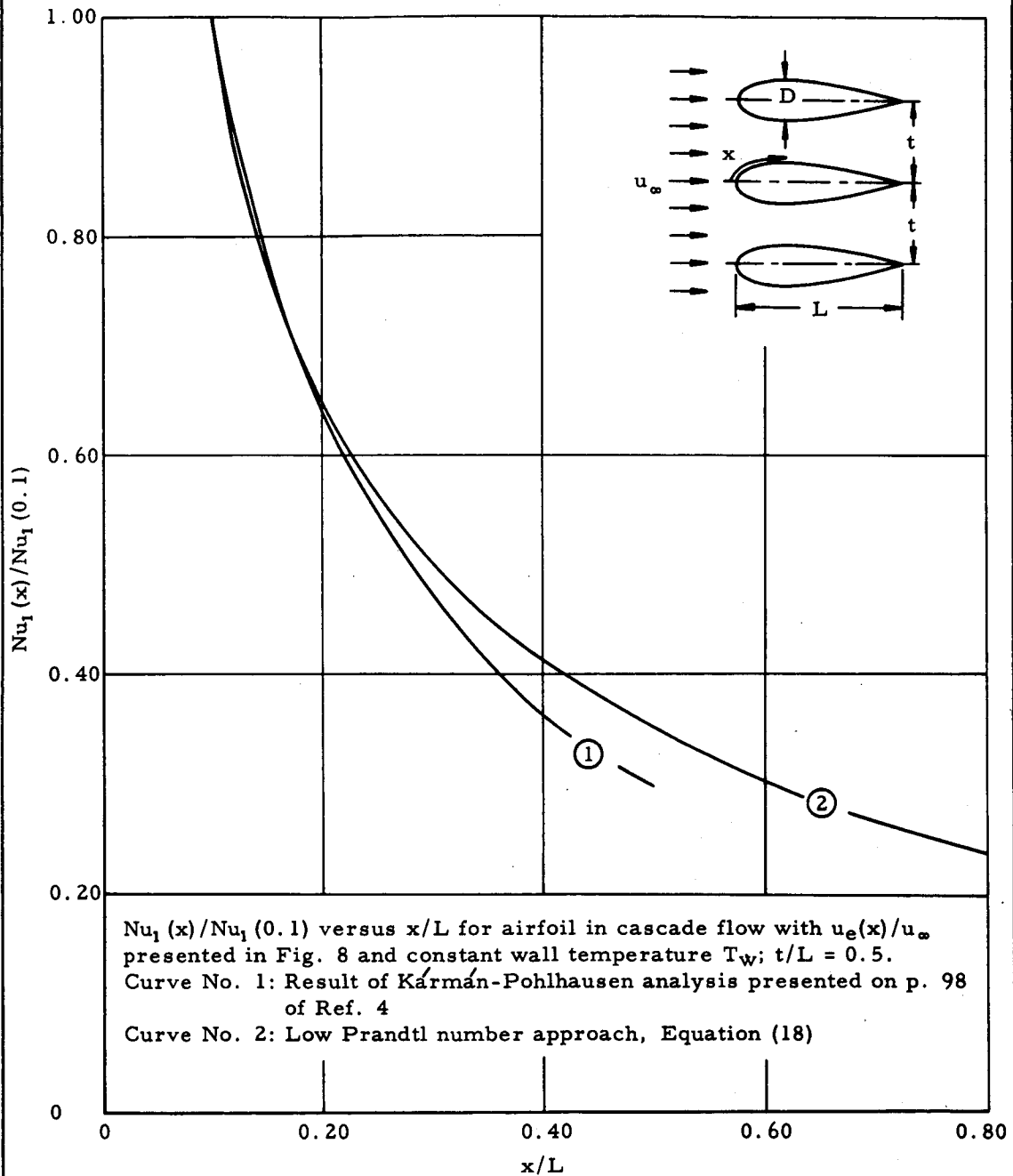


FIG. 15. $Nu_1(x)/Nu_1(0.1)$ FOR AIRFOIL IN CASCADE,
 $T_w = \text{CONST.}$

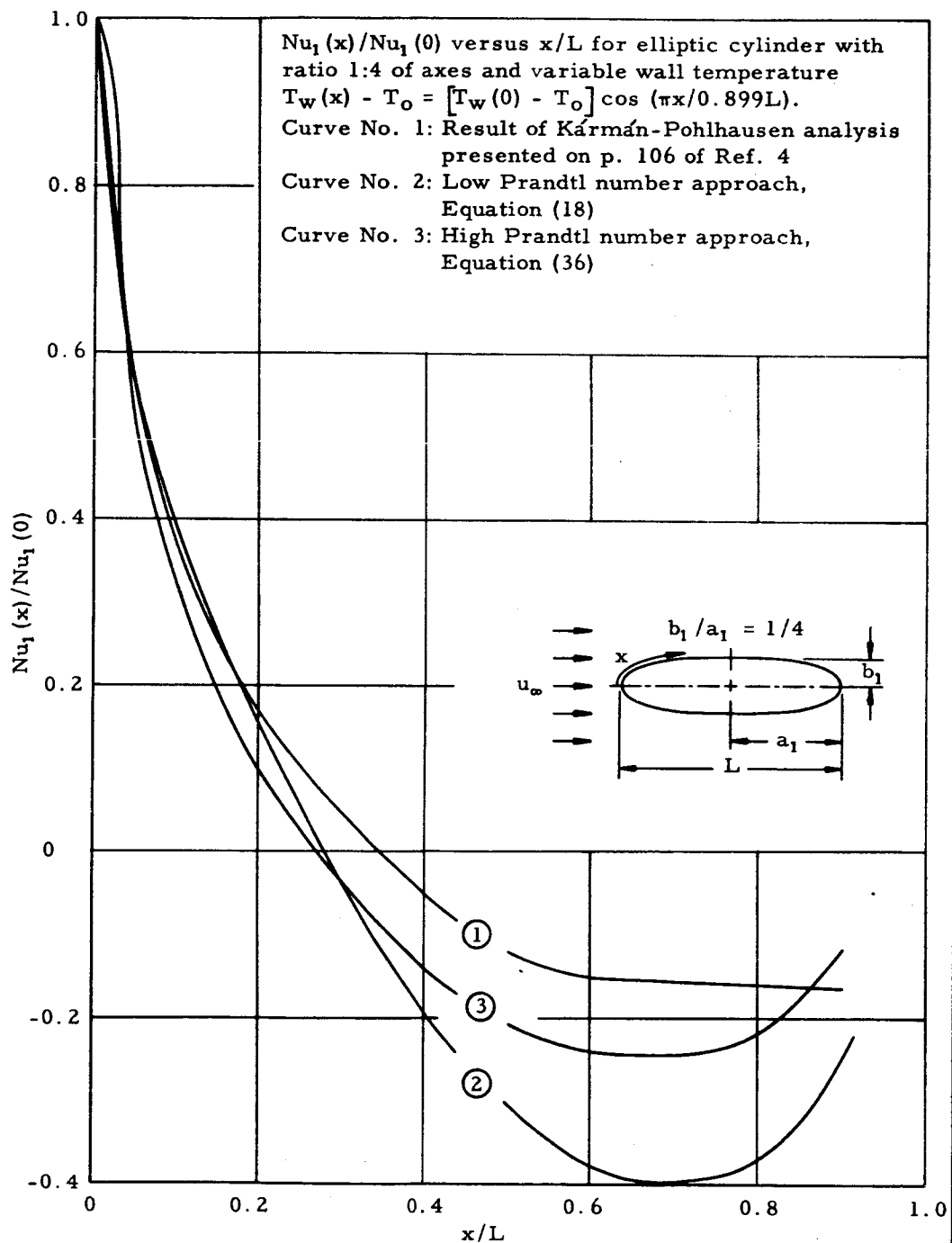


FIG. 16. $Nu_1(x)/Nu_1(0)$ FOR ELLIPTICAL CYLINDER 1:4, $T_w \neq \text{CONST.}$

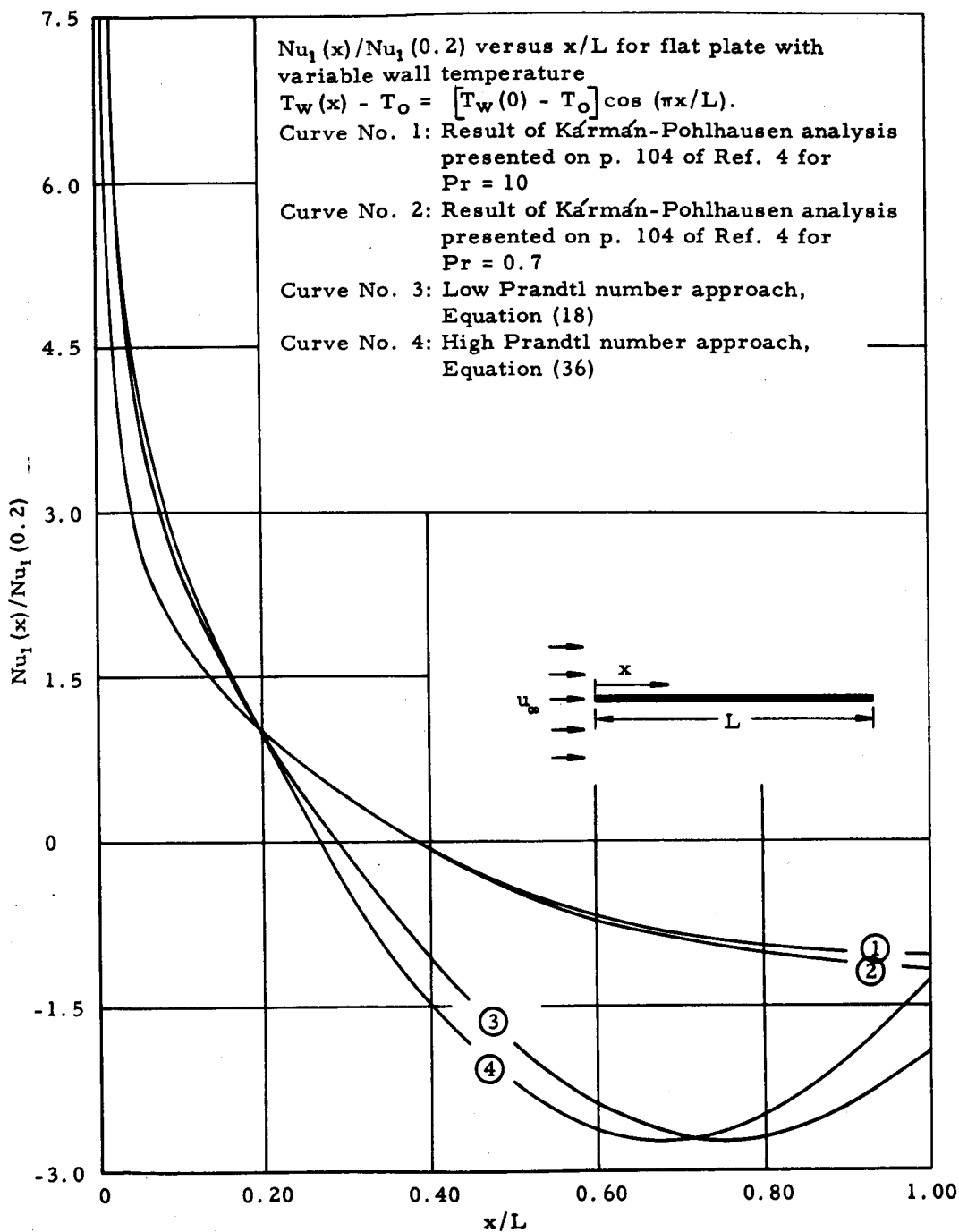


FIG. 17. $Nu_1(x)/Nu_1(0.2)$ FOR FLAT PLATE, $T_w \neq \text{CONST.}$

$Nu_3(x)/Nu_3(0)$ versus x/L for flat plate with variable wall temperature
 $T_w(x)/T_o = 1.25 - 0.83x/L + 0.33(x/L)^2$, where $Nu_3(x) = xq_w(x)/kT_o$.

Curve No. 1: Result of exact series expansion of solution on p. 561 of
 Ref. 2

Curve No. 2: Low Prandtl number approach, Equation (12)

Curve No. 3: High Prandtl number approach, Equation (32)

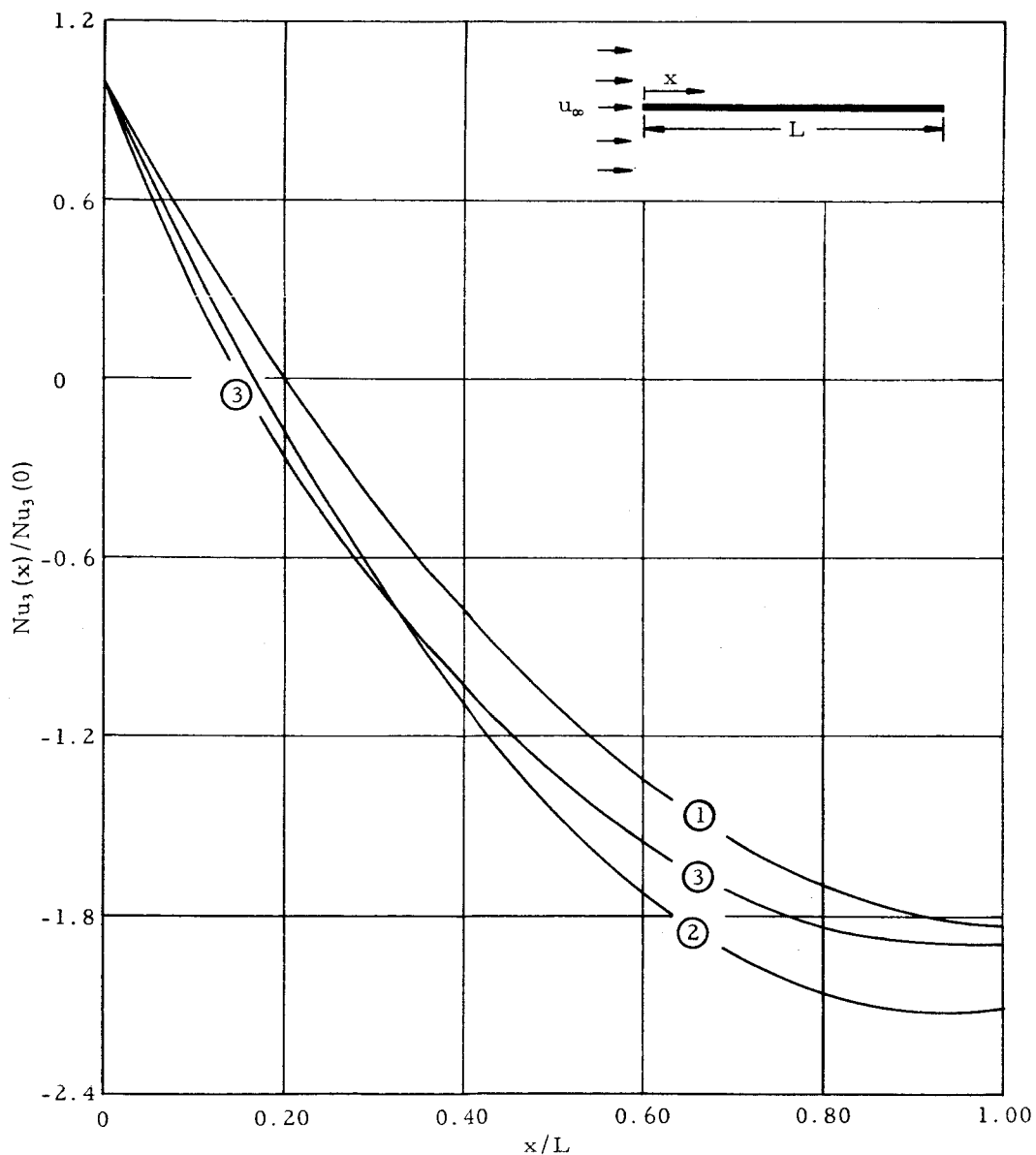


FIG. 18. $Nu_3(x)/Nu_3(0)$ FOR FLAT PLATE, $T_w \neq \text{CONST.}$

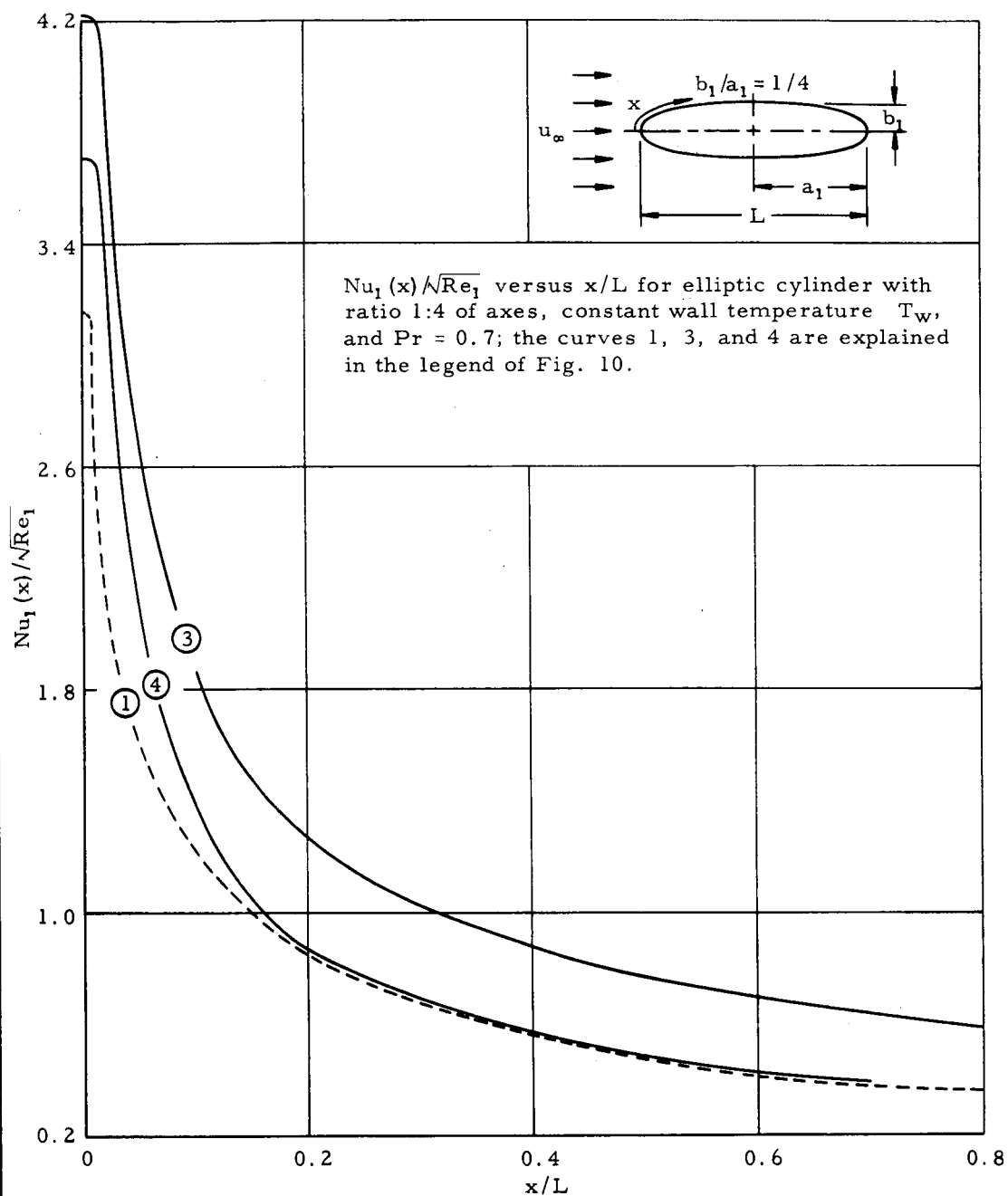


FIG. 19. $Nu_1(x)/\sqrt{Re_1}$ FOR ELLIPTICAL CYLINDER 1:4,
 $T_w = \text{CONST.}$

$Nu_1(x)/\sqrt{Re_1}$ versus x/L for circular cylinder with constant wall temperature T_w , and $Pr = 0.7$; the curves 1, 3, and 5 are explained in the legend of Fig. 13.

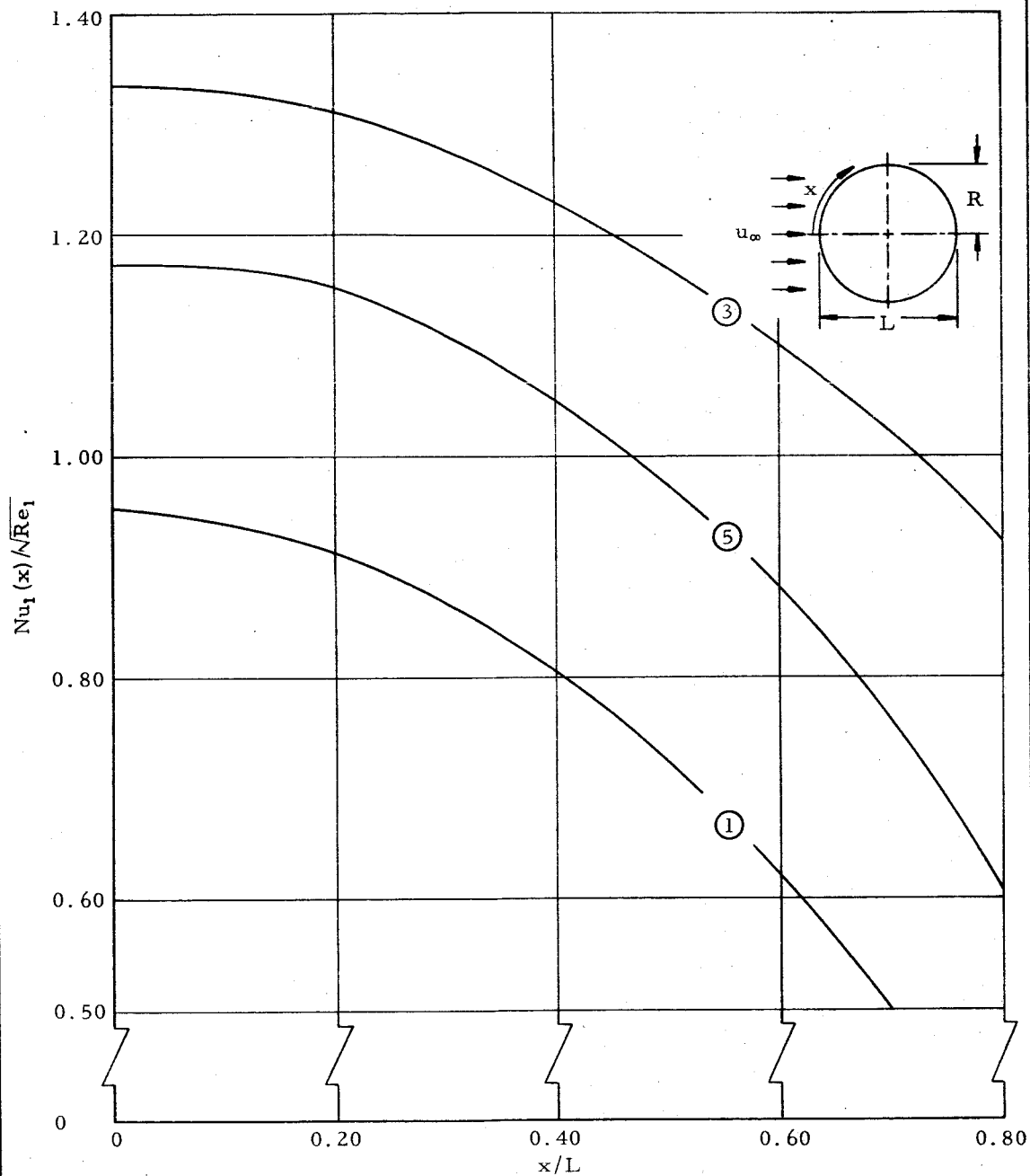


FIG. 20. $Nu_1(x)/\sqrt{Re_1}$ FOR CIRCULAR CYLINDER,
 $T_w = \text{CONST.}$

REFERENCES

1. Carslaw, H. S., and J. C. Jaeger, Conduction of Heat in Solids, Oxford University Press, Second Edition, London, 1959.
2. Chapman, D. R., and M. W. Rubesin, Temperature and Velocity Profiles in the Compressible Laminar Boundary Layer with Arbitrary Distribution of Surface Temperature, J.Ae.Sc., vol. 16, 1949, p.547.
3. Curle, N., Heat Transfer Through a Constant Property Laminar Boundary Layer, A.R.C., 22,584, F.M.3054, Feb. 1961.
4. Dienemann, W., Berechnung des Wärmeüberganges an laminar umströmten Körpern mit konstanter und ortsveränderlicher Wandtemperatur, ZAMM, vol. 33, 1953, p. 89.
5. Donoughe, P. L., and J. N. B. Livingood, Exact Solutions of Laminar-Boundary Layer Equations with Constant Property Values for Porous Wall with Variable Wall Temperature, NACA Tech. Rep. TR 1229, Washington, 1955.
6. Eckert, E. R. G., and R. M. Drake, Jr., Heat and Mass Transfer, McGraw-Hill Book Co., New York, 1959.
7. Frank, P., and R. v. Mises, Die Differentialgleichungen und Integralgleichungen der Mechanik und Physik, vol. 2, Second Edition, Dover Publications, New York, 1961.
8. Frössling, N., Evaporation, Heat Transfer, and Velocity Distribution in Two-Dimensional and Rotationally Symmetrical Laminar Boundary-Layer Flow, NACA Tech. Memo. TM 1432, Washington, Feb. 1958.
9. Hartree, D. R., On an Equation Occurring in Falkner and Skan's Approximate Treatment of the Equations of the Boundary Layer, Proc. Cambr. Phil Soc., vol. 33, part II, 1937, p. 223.
10. Levy, S., Heat Transfer to Constant-Property Laminar Boundary-Layer Flows With Power-Function Free-Stream Velocity and Wall-Temperature Variation, J.Ae.Sc., vol. 19, 1952, p. 341.
11. Liepman, H. W., A Simple Derivation of Lighthill's Heat Transfer Formula, J. Fluid Mechanics, vol. 3, 1958, p. 357.
12. Lighthill, M. J., Contributions to the Theory of Heat Transfer Through a Laminar Boundary Layer, Proc.Roy.Soc., A, vol. 202, 1950, p. 359.
13. Millsaps, K., and K. Pohlhausen, Thermal Distribution in Jeffery-Hamel Flows Between Non-Parallel Plane Walls, J.Ae.Sc., Vol. 20, 1953, p. 187.

REFERENCES (CONT'D)

14. Morgan, G. W., A. C. Pipkin, and W. H. Warner, On Heat Transfer in Laminar Boundary Layer Flows of Liquids Having a Very Small Prandtl Number, J.Ae.Sc., vol. 25, 1958, p. 173.
15. Pai, S., Viscous Flow Theory, Part I, D. Van Nostrand Co., Princeton, 1956.
16. Pohlhausen, K., Der Wärmeübergang zwischen festen Körpern und Flüssigkeiten mit kleiner Reibung und kleiner Wärmeleitung, ZAMM, vol. 1, 1921, p. 115.
17. Schlichting, H., Der Wärmeübergang an einer längsangeströmten ebenen Platte mit veränderlicher Wandtemperatur, Forsch. Ingenieurwesen, vol. 17, 1951, p. 1.
18. Schlichting, H., and E. Truckenbrodt, Aerodynamik des Flugzeuges, Springer, Berlin, 1959.
19. Schlichting, H., Boundary Layer Theory, Pergamon Press, London, 1955.
20. Spalding, D. B., Heat Transfer From Surfaces of Non-Uniform Temperature, J. Fluid Mechanics, vol. 4, 1958, p. 22.
21. Sparrow, E. M., Analysis of Laminar Forced-Convection Heat Transfer in Entrance Region of Flat Rectangular Ducts, NACA Tech Note TN 3331, 1955.
22. Sparrow, E. M., and J. L. Gregg, Details of Exact Low Prandtl Number Boundary Layer Solutions for Forced and for Free Convection, NASA Memo 2-27-59-E, Washington, 1959.
23. Squire, H. B., Heat Transfer Calculations for Aerofoils, ARC R&M 1986, 1942.

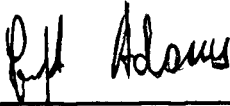
APPROVAL

MTP-AERO-62-19

THE LOW AND THE HIGH PRANDTL NUMBER APPROACHES FOR HEAT TRANSFER IN
LAMINAR FLOW OF INCOMPRESSIBLE FLUIDS
WITH CONSTANT MATERIAL PROPERTIES

ERNST W. ADAMS


The information in this report has been reviewed for security classification. Review of any information concerning Department of Defense or Atomic Energy Commission programs has been made by the MSFC Security Classification Officer. This report, in its entirety, has been determined to be unclassified.



ERNST W. ADAMS
Chief, Fluid Dynamics Section



WERNER K. DAHM
Chief, Aerodynamics Analysis Branch



E. D. GEISSLER
Director, Aeroballistics Division

DISTRIBUTION

M-MS-IP

M-MS-IPL (8)

M-CD

Mr. Eubanks

M-AERO

Dr. Geissler

Dr. Heybey

Mr. Bauer

Mr. Dahm

Mr. Wilson

Mr. Warmbrod

Mr. Berry

Mr. Huffaker

Mr. Fox (2)

Dr. Adams (25)

Dr. John A. O'Keefe
Assistant Chief
Theoretical Division
Goddard Space Flight Center
Greenbelt, Maryland

Dr. Dean R. Chapman
Aeronautical Research Scientist
Ames Research Center
Moffett Field, California

Mr. Joseph M. Spiegel
Research Specialist
Engineering Research Section
Jet Propulsion Laboratory
4800 Oak Grove Drive
Pasadena 3, California

M-MS-H

M-PAT

Mr. John Warden

HMEP